Geobios 51 (2018) 31–49

Available online at
ScienceDirect
www.sciencedirect.com

Elsevier Masson France
EM|consulte
www.em-consulte.com

Original article

A late Pleistocene skeleton of *Rhinoceros unicornis* (Mammalia, Rhinocerotidae) from western part of Thailand (Kanchanaburi Province)☆

Arnaud Filoux *, Varavudh Suteethorn

Palaeontological Research and Education Centre, Mahasarakham University, 44150 Mahasarakham, Thailand

ARTICLE INFO

Article history:
Received 12 June 2017
Accepted 20 December 2017
Available online 28 December 2017

Keywords:
Rhinocerotidae
Morphology
Biometry
Southeast Asia
Taphonomy

ABSTRACT

A subcomplete skeleton of a rhinoceros was discovered during excavation works in Kanchanaburi Province (Thailand) in May 1991. Fossil bones were preserved in anatomical connection in a late Pleistocene clay deposit. We describe these remains and refer them to as the Indian rhinoceros *Rhinoceros unicornis*. This fossil skeleton is the only one of its kind discovered in Southeast Asia and allows a complete description of the skeletal morphology of this species. The metric data reveal a close skeletal morphology with extant specimens from India and Nepal. The Kanchanaburi rhinoceros specimen confirms the much broader geographic distribution of the greater one-horned rhino during late Pleistocene times. This discovery provides a useful benchmark for the study of the evolutionary stages of this species in Southeast Asia during the concerned time interval.

1. Introduction

Rhinocerotids were abundant and diverse during the Pleistocene and the first part of the Holocene in southern Asia (Antoine, 2012). The three endangered species *Rhinoceros unicornis*, *Rhinoceros sondaicus* and the two-horned rhinoceros *Dicerorhinus sumatrensis* were more widespread during the past than today where they are restricted to some small, protected parks. In Thailand, only a few rhinoceros remains, limited to isolated bones or teeth, have been described in both Pleistocene paleontological and archeological sites. Some rhinoceros remains, mostly teeth, have been found in middle Pleistocene sites at Tham Wiman Nakin (Tougard, 1998) and Khok Sung (Suraprasit et al., 2016), in the late Pleistocene sites of Tham Prakai Phet (Tougard, 1998; pers. obs.), Cave of the Monk (Zeitoun et al., 2010), Tham Lod Rockshelter (Wattanapituksakul, 2006), Moh Kiew II (Auetrakulvit, 2004), and at Holocene sites of Khao Krim (Filoux, 2013), Ban Kao (Hatting, 1967), Khao Phanom Di (Higham and Thosarat, 2004), and Ban Non Wat (Thosarat and Kijngam, 2011). Referral to species is not always proposed for some of these sites. In Thailand, *Rhinoceros unicornis* remains are found associated with other rhinoceros species (*R. sondaicus* or *D. sumatrensis*). It has been identified at Khok Sung (*R. unicornis*; Suraprasit, 2016), at Tham Wiman Nakin (*R.* cf. *unicornis*; Tougard, 1998), and at Ban Fa Suai (*R.* cf. *unicornis*; Zeitoun et al., 2010). This species belongs to the Southeast Asian megafauna (related to large-bodied mammals > 44 kg *sensu* Martin, 1984) that is usually known as the *Stegodon-Ailuropoda* faunal complex characteristic of the Pleistocene (Kahlke, 1961; Colbert and Hooijer, 1953).

Few Pleistocene sites with mammal assemblages (other than micromammals) are known in Thailand, but a regional loss of megafauna at the transition of the late Pleistocene and Holocene is visible, with the disappearance of many taxa such as rhinoceros, giant panda, orangutan, and spotted hyena. Even if some of those taxa still persist somewhere in the biogeographic region, they occupy less than 10% of their maximum Holocene ranges and an even smaller percentage of their maximum Pleistocene ranges (Corlett, 2010). So far, the specimen collected in the Kanchanaburi Province is the most complete specimen of *Rhinoceros unicornis* discovered both in Thailand and in Southeast Asia. The present study provides a detailed description of this specimen and especially the well-preserved postcranial elements.

☆ Corresponding editor: Pierre-Olivier Antoine.

* Corresponding author.
E-mail address: filoux_arnaud@yahoo.fr (A. Filoux).

https://doi.org/10.1016/j.geobios.2017.12.003
0016-6995/

2. Geographical and geological settings

The subcomplete skeleton of *Rhincoceros unicornis* studied here was discovered in May 1991, in the small village of Yang Muang (Tha Maka district), 35 km to the East of Kanchanaburi city in the western part of Thailand. The discovery took place during excavations for a private building. The skeleton was removed by the owner and local people. The extraction took one day and was supervised by one of us (V.S.). The Kanchanaburi Province is situated in the Western part of Thailand, at the foot of the western mountain ranges. The landforms are dominated by mountains and hills in contact with the peneplain.

The Quaternary deposits in this area are the result of the transport of alluvium from the highlands and from the drainage of small intermontane basins. The Mae Klong River, which is the main river of the Western part of Thailand (Milliman et al., 1995), flows from the Tenasserim Hills and creates an alluvial fan (Fig. 1). The Kanchanaburi area is dominated by the apex of the Kamphaeng-saen fan delta that spreads eastward (Jarupongsakul et al., 1991). The area consists of river deposits, predominantly gravel beds alternating with sand, silt, and clayey layers and clay-rich loam with some iron-oxide pisolites (Jarupongsakul et al., 1991; Takaya, 1972; Alekseev and Takaya, 1967). The specimen was embedded in a clay deposit at a depth of 4 meters in contact with a gravel bed (as observed on photography taken during the excavation process; Fig. S1, Appendix A).

As no stratigraphic study has been conducted, we will attempt to correlate the deposit with local stratigraphy. One of the outcrops studied and analyzed by Takaya (1972), locality 182, is 7 km away from the site. We use this sedimentary sequence to assess the possible age of the skeleton. Carbon dating analysis has been performed on two rib fragments, but the lack of collagen in the bone does not permit for getting a radiometric age for the specimens. We assume that the gravel bed found at the base of the excavation, at *ca.* 4 m depth, is in contact with the rhinoceros remains and corresponds to Takaya's (1972) layer 5 or one of the surrounding layers. Even though lateral variations are important in alluvial fans because of innumerable repetitive changes in the old river course and overflow flooding (Jarupongsakul et al., 1991), we assume that the skeleton was discovered in Formation II and is most probably late Pleistocene in age (Dheeradilok, 1995).

3. Material and methods

The fossil specimens from Kanchanaburi correspond to one individual. All the remains are housed in the collection of the Sirindhorn Museum (Kalasin Province, Thailand). The terms and the diagnosis key are taken from Guérin (1980) and Antoine (2002). Measurements are taken with a digital caliper in mm, using the bone and tooth measuring methodology of Guérin (1980). The most diagnostic postcranial remains are compared with other Asian rhinoceros fossils (Hooijer, 1946; Beden and Guérin, 1973; Yan et al., 2016) and extant rhinoceros materials (Guérin, 1980) using Simpson's (1941) log-ratio diagram method with extant *Diceros bicornis* (Guérin, 1980) as reference. A profile gauge was used to figure out the outlines of the upper teeth (at 2.5 cm from the neck of the teeth) and the mid-section diaphysis of the metapodials following Guérin (1980).

4. Systematic paleontology

Class Mammalia Linnaeus, 1758
Order Perissodactyla Owen, 1848
Family Rhinocerotidae Gray, 1821
Subfamily Rhinocerotinae Gray, 1821
Tribe Rhinocerotini Gray, 1821
Genus ***Rhinoceros*** Linnaeus, 1758
Rhinoceros unicornis Linnaeus, 1758
Figs. 2–8

Referred specimen: An almost complete skeleton from Kanchanaburi Province Thailand. The remains are stored at the Sirindhorn Museum, Kalasin Province, Thailand.

Description:

Cranial elements.

Skull. The skull is poorly preserved and incomplete: only the palate, the left jugal bone, the left zygomatic arch (Fig. 2(A, B)), a small part of the frontal, and an incomplete parietal are preserved. The skull retains the M1 and M2 on both sides. The P4 and the M3

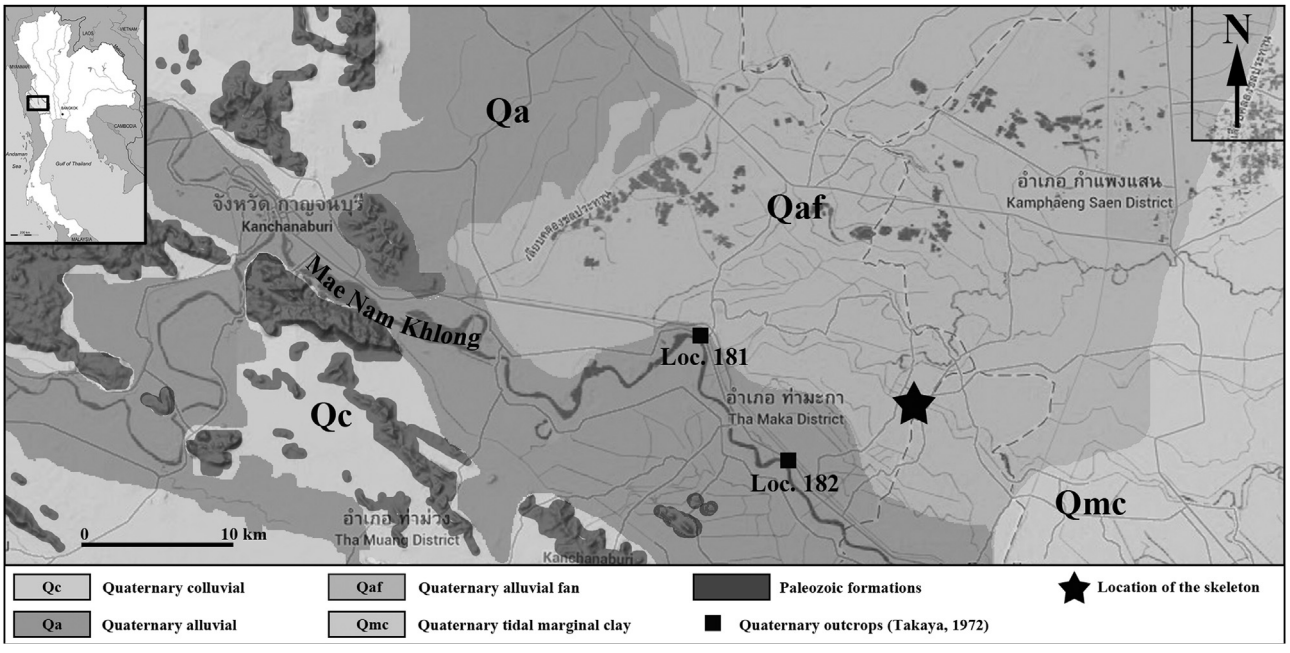

Fig. 1. Geological map of the Kanchanaburi area (Thailand), showing the development of the alluvial fan and the location of the fossil skeleton of *Rhinoceros unicornis*.

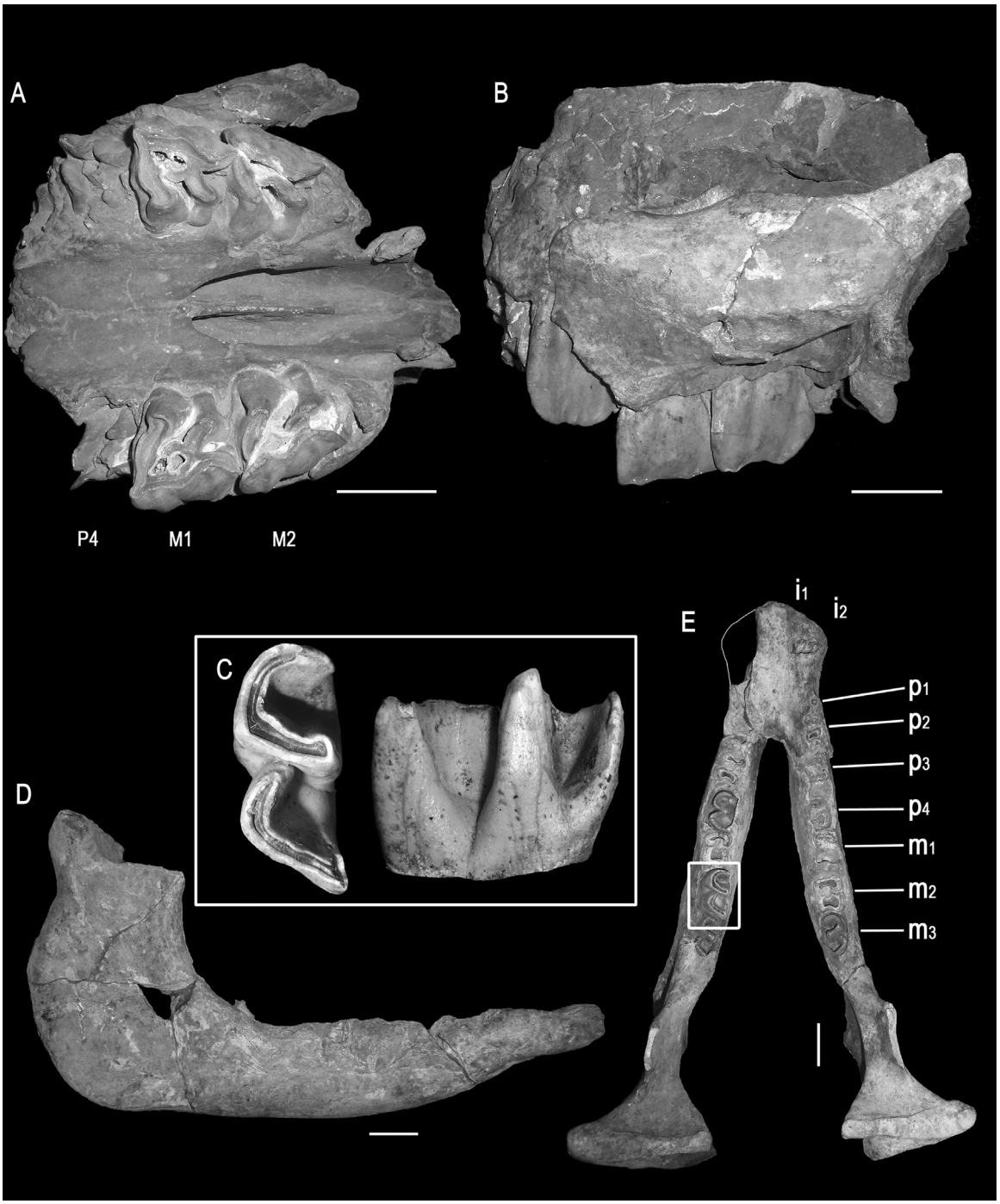

Fig. 2. *Rhinoceros unicornis* from Kanchanaburi (Thailand). **A, B.** Fragmented skull in ventral (A) and lateral (B) views. C. Lower left m2 in occlusal and lingual view. **D, E.** Mandible in lateral (D) and dorsal (E) views. Scale bars: 5 cm.

are formed but are not erupted from the maxillary. The ventral view (Fig. 2(A)) shows a palatal surface with a narrow mid-ridge in the longitudinal axis of the skull. The presence of foramina along the suture between the maxillary and the palatal are observed. The posterior border of the palate lies between M1 and M2.

Mandible. The mandible is well preserved and nearly complete (Fig. 2(D, E)). The mandibular symphysis is visible, long and lightly oblique in lateral view. The inferior border presents a straight and slightly oblique outline in the anterior part. Two small mental foramens are present at the p2 level. The posterior part of the symphysis is close to the posterior part of the p2. The ventral part of the symphysis is slightly depressed. The mandibular foramen is at the alveolar border level. The anterior part of the mandible shows the roots of the central incisor (i1). Only the right alveolus of the lateral incisors (i2) is well preserved and wider than the alveolus of the i1. The crown of the incisor is missing; only the right i2 root is retained in the alveolus by a fragment which shows a sub-oval section and a development far back to the lingual side of the p2.

Upper dentition. The M1 presents a nearly trapezoidal outline. The ectoloph is slightly undulating (Fig. 2(A); Fig. S2, Appendix A). The paracone and the metacone ribs are slightly marked. The parastyle fold is absent. Although small, the crista is simple and

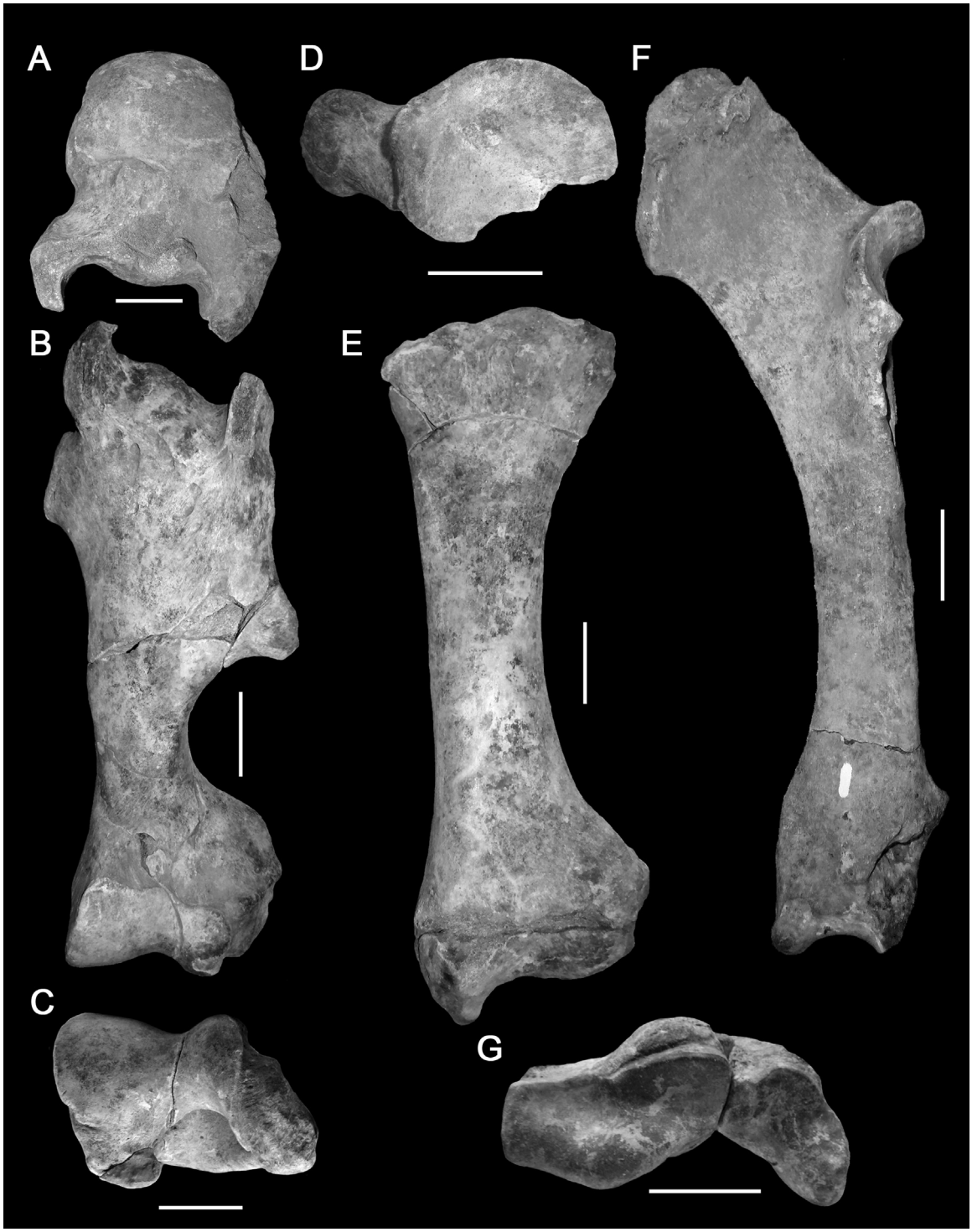

Fig. 3. Skeletal elements of the forelimbs of *Rhinoceros unicornis* from Kanchanaburi (Thailand). **A-C.** Left humerus in proximal (A), anterior (B), and distal (C) views. **D.** Left scapula in distal view. **E.** Left radius in anterior view. **F.** Left ulna in medial view. **G.** Radius-ulna articular complex in distal view. Scale bars: 5 cm.

present on both specimens. The crochet is present, strong and digitate on the right specimen. The angle between the crochet and the metaloph is acute. Some enamel folds are present on the posterior part of the protoloph. The medifossette is nearly closed on the left M1 and closed on the right M1. On the anterior face a small anterior cingulum, continue and oblique with a sinusoidal shape is present. The protocone constriction is well marked on both specimens. The M2 are less worn than the M1 and the protoloph is not linked to the paracone. They present larger dimensions. The paracone and the metacone are not so developed and the protocone constriction is weak. The crista is not visible.

Lower dentition. Only the left m2 is preserved and can be analyzed (Fig. 2(C)); the left p4 and both m3 are not erupted and cannot be described. The m2 shows an anterior valley with a V-shape and a large V-shape for the posterior valley. The difference of height between the two valleys is low. The tooth is narrow. The external syncline on the buccal face of the m2 is open and shallower at the tooth neck.

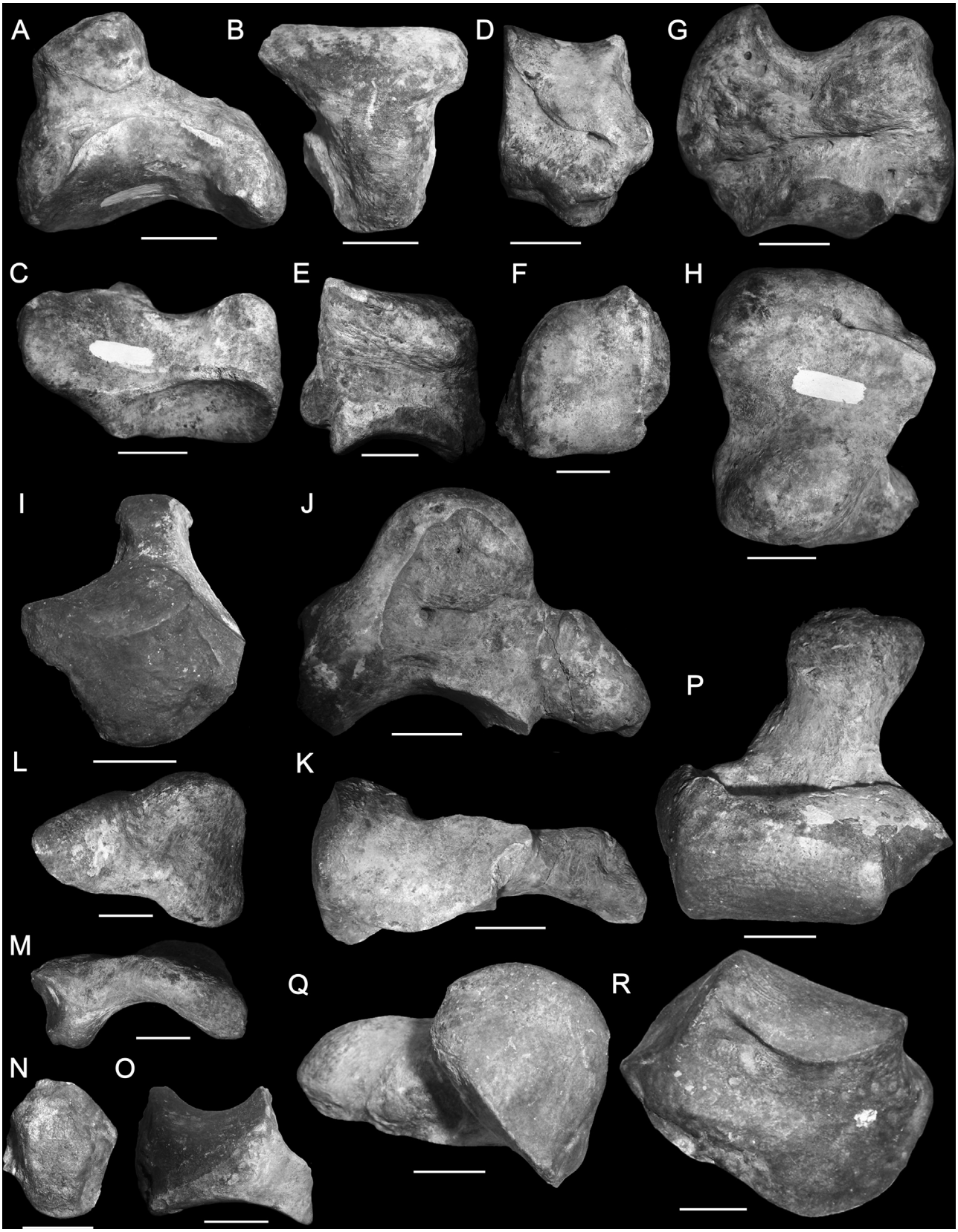

Fig. 4. Carpal elements of *Rhinoceros unicornis* from Kanchanaburi (Thailand). **A-C.** Left semi lunar in lateral (A), anterior (B), and distal (C) views. **D-F.** Left pyramidal in posterolateral (D), posteromedial (E), and distal (F) views. **G, H.** Left scaphoid in anterior (G) and proximal (H) views. **I-K.** Left magnum in anterior (I), lateral (J), and distal (K) views. **L, M.** Pisiform in lateral (L) and distal (M) views. **N, O.** Trapezoid in anterior (N) and lateral (O) views. **P-R.** Left uncinate in proximal (P), medial (Q), and anterior (R) views. Scale bars: 2 cm.

Post cranial elements.

Scapula. The scapulas are poorly preserved, with fragmentary blades. The glenoid cavity shows an oval shape with the proximal edge straight; the medial ridge is broken (Fig. 3(D)). The supraglenoid tuber is massive.

Humerus. The humerus shows a proximal epiphysis with a wide and shallow bicipital groove. The preservation of the bones does not allow the full observation of the elongated and medially hooked greater tubercle (Fig. 3(A)). The deltoid tuberosity is strongly developed laterally (Fig. 3(B)). The diaphysis exhibits on the posterior face a nutrient foramen. The anterior face of the distal epiphysis shows a large and shallow coronoid fossa. The lateral epicondyle is large and massive and its posterior development is as much as the medial epicondyle. The posterior face shows a wide, deep and low elliptic olecranon fossa. A distal gutter on the lateral epicondyle is present (Fig. 3(C)).

Radius. The radius presents a proximal epiphysis with an anterior edge nearly straight; the lateral articular surface for the humerus is strongly developed transversally. The posterior edge of the external surface shows a strong obliquity. On the posterior part, the two articular facets for the ulna are fused. The diaphysis shows a clear asymmetry between the lateral and medial edges, the former being more arched than the latter (Fig. 3(E)). In lateral view, a well-marked crest is developed on the distal part of the diaphysis. The distal epiphysis presents a strong styloid process and the posterior expansion of the facet for the scaphoid is low vertically.

Ulna. The ulna is arched; the angle between the shaft and the olecranon is acute (Fig. 3(F)). The latero-external tuberosity of the olecranon is curved inward, making a strongly convex medial face. On the proximal epiphyses, the articular facets for the radius are fused; the obliquity of the articular surface is not important. The diaphysis shows a triangular outline. The distal epiphysis shows a marked depression on the antero-internal face, and the lateral face shows a heavy prominence. The articular surface for the pyramidal is concave; a small articular facet for the semi-lunar is present (Fig. 3(G)).

Semilunar. The anterior face of the semilunar has an open V-shape slightly bent medially with a distal squared tip (Fig. 4(B)). The superior face presents the articular surface for the radius on the anterior part, and a small articular facet for the ulna on the lateral part. In medial view, the proximal articular surface for the scaphoid occupies the complete length of the face, and on the distal part a small facet for the scaphoid is marked. On the lateral face the small facet for the pyramidal is in contact with the facet for the ulna; the distal facet for the pyramidal is long and present a semi-elliptical shape (Fig. 4(A)). The uncinate and magnum facet are separated by a marked crest (Fig. 4(C)).

Pyramidal. The pyramidal presents a trapezoidal articular surface for the ulna, with an anterior edge longer than the posterior (Fig. 4(D)). The articular surfaces for the semilunar are separated by a horizontal depression (Fig. 4(E)). The proximal facet does not extend to the posterior part of the face. The distal facet is a stripe with a higher lateral development. In distal view the articular surface for the uncinate is squared (Fig. 4(F)).

Scaphoid. The height difference between the anterior and the posterior part of the scaphoid is not marked (Fig. 4(G)). On the proximal face, the articular surface for the radius is concave, deep and stretched antero-posteriorly, with a trapezoidal outline (Fig. 4(H)). The distal face presents two main articular facets (for the magnum and trapezoid) and a small facet for the trapeze. On the medial face, a deep groove highlights the superior extension of the trapezoid facet. The lateral face shows a superior facet for the semilunar, continue and forming a large strip higher in the

Fig. 5. Metacarpals of *Rhinoceros unicornis* from Kanchanaburi (Thailand). **A, D, G, J.** Left second metacarpal in anterior (A), proximal (D), lateral (G), and medial (J) views. **B, E, H, K.** Left third metacarpal in anterior (B), proximal (E), lateral (H), and medial (K) views. **C, F, I, L.** Left fourth metacarpal in anterior (C), proximal (F), lateral (I), and medial (L) views. Scale bars: 5 cm.

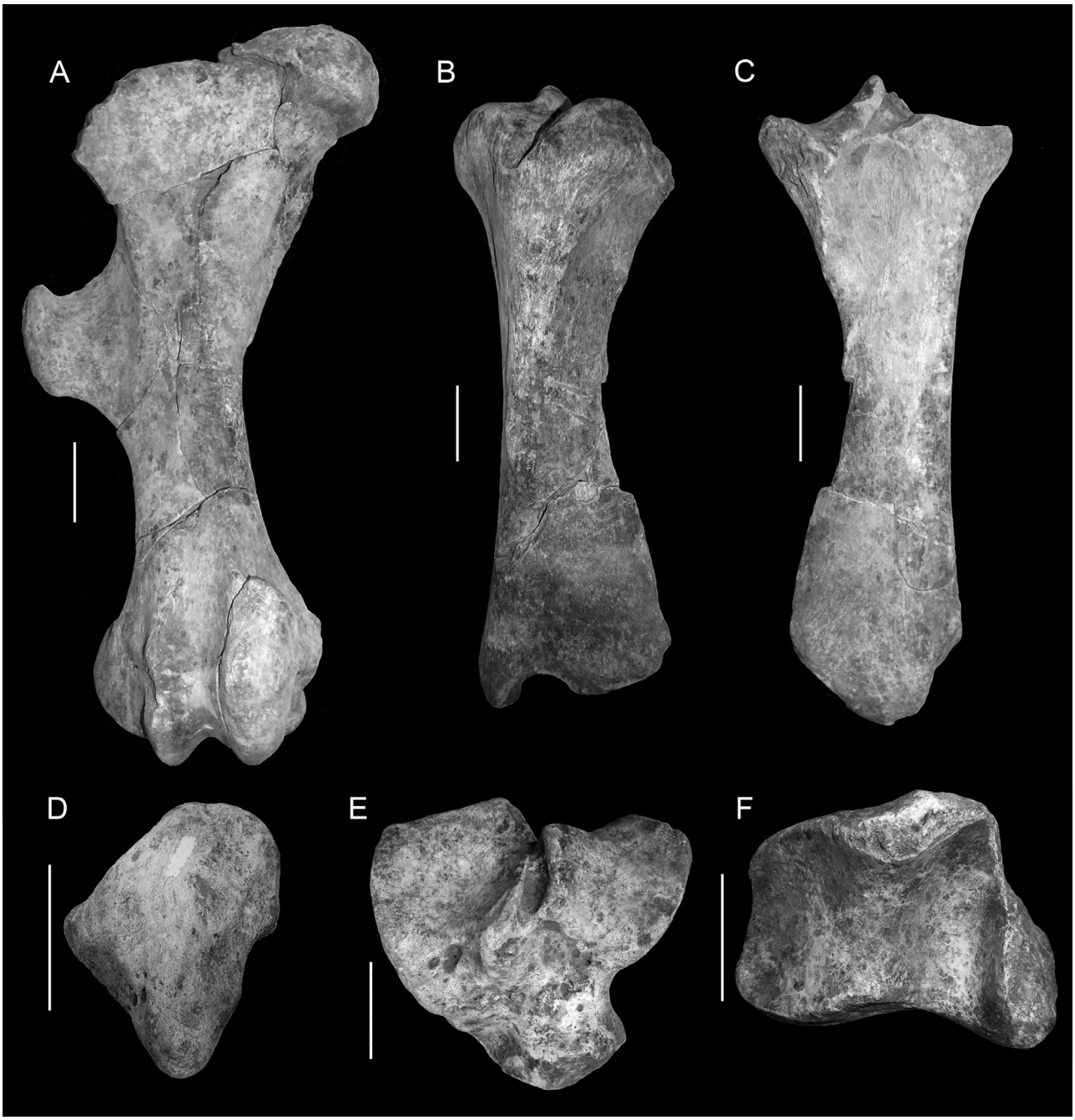

Fig. 6. Skeletal elements of the hindlimbs of *Rhinoceros unicornis* from Kanchanaburi (Thailand). **A.** Right femur in anterior view. **B, C, E, F.** Left tibia in anterior (B), posterior (C), proximal (E), and distal (F) views. **D.** Right patella in anterior view. Scale bars: 5 cm.

posterior part, and a distal facet for the semilunar with a crescent form in contact with the magnum facet.

Magnum. In anterior view, the magnum has a pentagonal shape (Fig. 4(I)), with a strong transverse medial development. In lateral view (Fig. 4(J)), the dorso-medial surface for the scaphoid gradually shifts to the facet for the trapezoid. A second facet corresponding to the second metacarpal is separated from the former by a small depression. The posterior tuberosity is well developed. The distal face (Fig. 4(K)) is composed by the articular surface for the third metacarpal; it is wide and long, presenting a convex lateral edge and a nearly straight medial edge with a small concavity on the medial part.

Pisiform. The pisiform show on the anterior face the articular facets for the ulna and the pyramidal, separated by a rounded crest. The posterior face is higher than the anterior one (Fig. 4(L)), and the medial face presents a strong concavity (Fig. 4(M)).

Trapezoid. The trapezoid presents a proximal face totally formed by a squared articular surface with a strong antero-posterior convexity. The posterior face presents a vertical depression. In lateral view, the articular surface for the magnum occupies the majority of the face and progressively passes on the distal part to the second metacarpal facet (Fig. 4(O)). On the medial face the articular surface for the trapeze is delimited anteriorly by a small depression. In distal view, the facet for the second metacarpal is elliptical with a posterior tip.

Uncinate. The uncinate presents an anterior face with a lateral edge slightly higher than the medial one (Fig. 4(R)). On the medial view the facet for the semilunar is regularly convex, high and

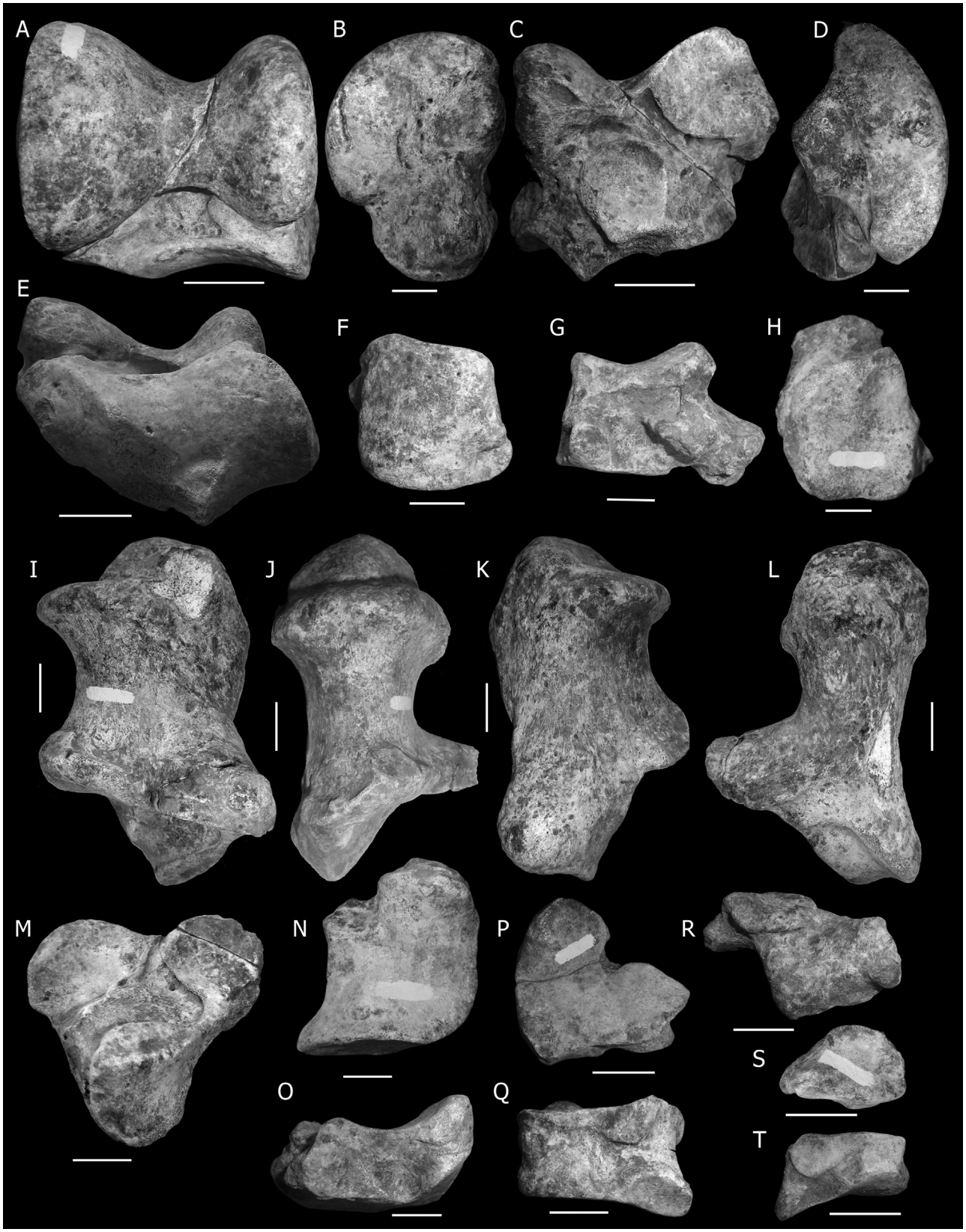

Fig. 7. Tarsal bones of *Rhinoceros unicornis* from Kanchanaburi (Thailand). **A-E.** Right astragalus in anterior (A), medial (B), posterior (C), lateral (D), and distal (E) views. **F-H.** Right cuboid in anterior (F), medial (G), and proximal (H) views. **I-M.** Right calcaneum in medial (I), anterior (J), lateral (K), posterior (L), and distal (M) views. **N, O.** Right navicular in proximal (N) and lateral (O) views. **P, Q.** Right third cuneiform in proximal (P) and lateral (Q) views. **R.** Right first cuneiform in lateral view. **S, T.** Right second cuneiform in proximal (S) and medial (T) views. Scale bars: 2 cm.

sub-triangular, and slightly overflows on the anterior part (Fig. 4(Q)). On the proximal face, the articular surface for the pyramidal is limited posteriorly by a small depression and laterally by the articular surface for the metacarpal V (Fig. 4(P)). A contact between the articular surface for the pyramidal and the metacarpal V exists.

Second metacarpal. The second metacarpal is nearly straight in anterior view (Fig. 5(A)). The proximal epiphysis is formed by a large articular surface for the trapezoid, with a hemi-circular shape mostly convex antero-posteriorly and concave latero-medially in the anterior part (Fig. 5(D)). Two distinct articular facets are present on the lateral face of the epiphysis (Fig. 5(G)). The biggest one corresponds to the articular surface for the magnum; it is long and presents a medial small concavity on its distal edge. The contact between the facet for the magnum and the metacarpal III is well marked; the angle made by the two facets is clearly visible. On the medial face a small facet for the trapeze is present (Fig. 5(J)). The diaphysis shows an elliptical medial section with a posterior part slightly more convex.

Third metacarpal. The third metacarpal is long, straight and flat (Fig. 5(B)). The proximal epiphysis is expanded transversely; the articular surface for the magnum appears trapezoidal with a lateral edge slightly depressed and overflowing on the anterior face (Fig. 5(B, E)). A very strong saliency separates the proximal articular surface and the facet for the uncinate. In lateral view the lateral surface has two distinct facet joints; the anterior facet is not complete on the right specimen but on the left specimen the complete articular complex is preserved (Fig. 5(H)). The two facets for the metacarpal IV are separated by a large groove; the posterior facet, located more distally than the anterior one, is large and presents a triangular shape with the proximal edge reaching the articular surface for the magnum. On the medial face the small triangular facet for the second metacarpal is present (Fig. 5(K)). The section of the shaft is elliptical, wide and flat with a sharper lateral edge (Fig. 9).

Fourth metacarpal. In anterior view, the fourth metacarpal is lightly arched (Fig. 5(C)). The proximal articular surface for the uncinate presents a hemi-circular shape with a strong convexity on the middle of the posterior edge (Fig. 5(F)). The medial face of the proximal epiphysis (Fig. 5(L)) is composed of two well-separated articular facets for the third metacarpal. The posterior facet is high and wide and presents an elliptical shape; the anterior facet is long and low and it is one third of the height of the posterior one, with a slightly oblique proximal edge. The articular facet for the fifth metacarpal is less pronounced but a small crest separates it from the uncinate facet (Fig. 5(I)). The section of the shaft is a regular ellipse (Fig. 9).

Fifth metacarpal. Only the left specimen is preserved; it shows a globular shape truncated by the uncinate articular surface.

Pelvis. The pelvis is badly preserved and the bones are too fragmented to propose a metric and morphological description.

Femur. The two femora are almost complete. On both specimens the proximal epiphysis is not fused. The head shows a hemispheric shape with a fovea well-marked, large and low. The diaphysis is flat and presents a well pronounced third trochanter on the lateral side (Fig. 6(A)). In anterior view, the distal extremity shows a medial ridge more developed than the lateral one; the proximal outline of the trochlea is not so pronounced, and a tiny fossa is visible above.

Patella. Both patellae are preserved and exhibit a quadrangular shape. The anterior face presents a strong distal tip (Fig. 6(D)). In posterior view the lateral facet is more developed than the medial one, and separated by a high and concave relief.

Tibia. The proximal articular surface shows a broad tibial tuberosity that slightly bent outward and is limited laterally by a tibial gutter well marked and medially by a clear digital fossa with

Fig. 8. Metatarsals of *Rhinoceros unicornis* from Kanchanaburi (Thailand). **A, D, G, J.** Right fourth metatarsal in anterior (A), proximal (D), medial (G), and lateral (J) views. **B, E, H, K.** Right third metatarsal in anterior (B), proximal (E), medial (H), and lateral (K) views. **C, F, I, L.** Right second metatarsal in anterior (C), proximal (F), medial (I), and lateral (L) views. Scale bars: 5 cm.

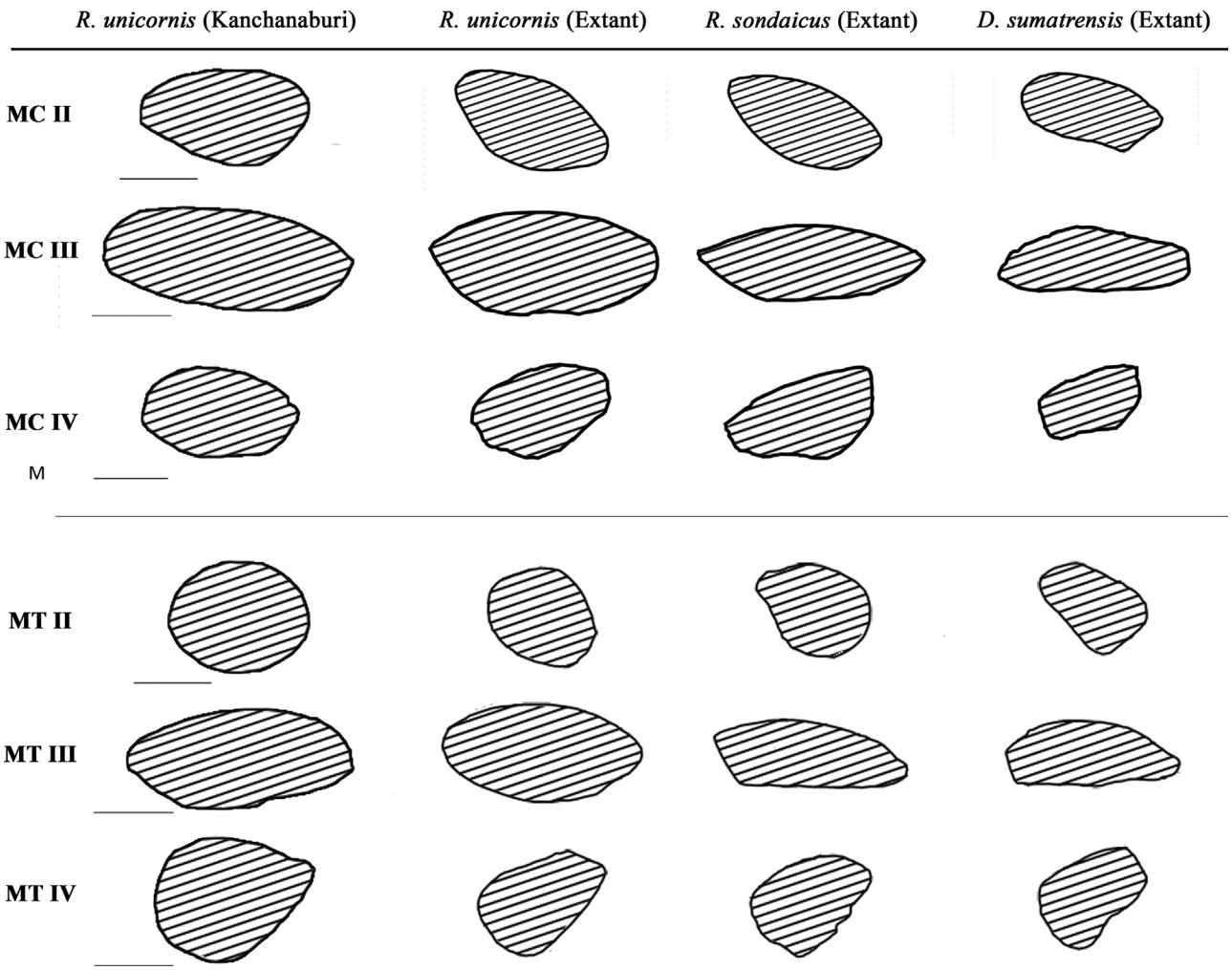

Fig. 9. Mid-diaphysis transverse section of metacarpals and metatarsals of *Rhinoceros unicornis* from Kanchanaburi (Thailand), compared with extant Asian representatives (Guérin, 1980). Scale bars: 2 cm.

a short distal extension (Fig. 6(E)). The caudal intercondylar area is less extended. The area between the two intercondylar eminences is poorly developed and shallows longitudinally. The two eminences are close to one another; the medial eminence is a little higher than the lateral one. The caudal face of the diaphysis presents a net but undeveloped popliteal line (Fig. 6(C)). The popliteal groove is slightly hollowed and a little extended transversely. The lateral edge is more arched than the medial one (Fig. 6(B, C)). The distal epiphysis presents a fibular notch barely marked and slightly drawn. The posterior apophysis is low and rounded (Fig. 6(C)). The medial malleole is strongly developed.

Fibula. Only the distal epiphysis of the fibula can be analyzed. We observe a deep and median, latero-distal coulisse and on the other side a broad articular surface for the tibia

Astragalus. The posterior edge of the astragalus trochlea is subrectilinear in proximal view. The anterior face has a broad and deep trochlea (Fig. 7(A)). The distal extension of the lateral lip is slightly more pronounced than the medial lip. A marked transverse deep depression limits the trochlea distally. On the posterior face (Fig. 7(C)), the proximo-lateral articular surface is concave and has a rounded square shape with a well-marked small distal extension. The medio-distal articular surface is circular to elliptical and fused with the latero-distal elliptical articular surface for the calcaneum. On the medial face the articular surface is well developed antero-posteriorly and shows a very circular curvature (Fig. 7(B)). The distal tubercle is well developed near the distal part and slightly shifted to the posterior edge. On the lateral view the articular surface for the tibia covers the majority of the face and presents a curved elliptical shape (Fig. 7(D)). The distal face shows a slightly obliquely concave anterior edge and a convex posterior edge. The facet for the cuboid is rectangular and the one for the navicular is trapezoidal (Fig. 7(E)).

Calcaneum. The specimens are robust with massive tuber calcanei with rough summit. In medial view the difference of height between the top of the bone and the anterior part of the tuber calcanei is important (Fig. 7(I)). In anterior view the articular facet for the tibia is clearly visible; the lateral and medial edge below the tuber calcanei appear nearly parallel (Fig. 7(J)). In lateral view the development of the anterior tip of the tuber calcanei is less important than the beak, the posterior border shows a slightly undulate shape (Fig. 7(K)). The fibula facet is small and less marked than the tibia one. In posterior view (Fig. 7(L)) the sustentaculum is thick, and the proximal edge makes an obtuse angle with the axis of the bone; the distal edge is weakly oblique. In distal view (Fig. 7(M)) the facet for the cuboid appears as a long and broad hemi-circular shape. The anterior face shows the articular facets for the astragalus. The articular facet placed on the sustentaculum has a rounded shape; it is fused with the more distal, elliptical sharped-shape facet. The third one is large and convex with its medial edge in contact with the facet for the tibia.

Cuboid. The bone shows a strong and long posterior tuberosity. The anterior face is nearly squared, slightly trapezoidal, with a

Table 1
Comparative measurements (in mm) of the teeth of *Rhinoceros unicornis* from Kanchanaburi (Thailand) and from extant and fossil Asian rhinoceros specimens.

	Fossil								Extant[h]		
	R. unicornis Kanchanaburi	*R. unicornis* Khok Sung[a]	*R. unicornis* Duoi U'Oi[b]	*R. sinensis* Yenchingkou[c]	*R. sinensis* Longgudong[d]	*R. sinensis* Paxian Dadong[e]	*R. kendengindicus* Kedung Brubus[f]	*R. sivalensis* Siwalik[g]	*R. unicornis*	*R. sondaicus*	*D. sumatrensis*
m2											
n	1	1	1	7	14		1	1			
L	53	50.74	50	49–61 (47.9)	43–51.5 (47.9)		48	50.8	52–56.5 (54.1)	40.5–51 (46.2)	39–47.5 (43.3)
W	32		29	29–37 (29.1)	25.8–35.5 (29.1)		30	30.5	31–36 (32.5)	27–32.5 (29.4)	23.5–28 (26.1)
M1											
n	2	1		10	7	6	3	1			
L	55–57 (56)	47.95		41–55 (49.3)	45.8–54.3 (49.3)	47.2 –55 (49.1)	42–44 (43.3)	44.6	48–58 (53.3)	46–51 (48.9)	46–51.5 (47.9)
Wa	65–68 (66.5)	70.5		63–81 (68.7)	53–69.5 (58.4)	54.4–67.8 (60.3)	58–65 (62.3)	66	62–72.5 (65.7)	52.5–60 (55.8)	46.5–54 (49.4)
Wp	61	58.8		59–76 (63.8)	49.5–60.7 (54.4)						
M2											
n	2			10	10	3	6	1			
L	61			45–60 (57.8)	46.8–57.8 (51.4)	50–52.6 (51.3)	42–47 (45.3)	50.8	53–62 (57.6)	44.5–55 (50.5)	47.5–55 (50.4)
Wa	67–68 (67.5)			63–82 (72.4)	53–65 (58.4)	45–58 (53.3)	61–66 (64.2)	66	64.5–76 (68.6)	53–62 (57.5)	48–57 (51.8)
Wp	58–60 (59)			56–75 (63.6)	47.5–56 (48.6)						

n: number of specimen; **L**: length; **Wa**: anterior width; **Wp**: posterior width, mean in brackets.
[a] Data from Suraprasit et al. (2016).
[b] Data from Bacon et al. (2008a).
[c] Data from Colbert and Hooijer (1953).
[d] Data from Zheng (2004).
[e] Data from Schepartz and Miller-Antonio (2008).
[f] Data from Hooijer (1946).
[g] Data from Falconer (1867), Lydekker (1881).
[h] Data from Guérin (1980).

Table 2
Comparative measurements (in mm) of forelimb bones of *Rhinoceros unicornis* from Kanchanaburi (Thailand) and from extant and fossil Asian rhinoceros specimens.

	Fossil			Extant[b]		
	R. unicornis Kanchanaburi		*R. sondaicus guthi* Phnom Loang[a]	*R. unicornis*	*R. sondaicus*	*D. sumatrensis*
	Left	Right				
Scapula						
DT neck	34	34		40	31–46	22.5–35
DAP tuber	160	161		163	117.5–152	98.5–106.5
DAP art.	99	100		96	70–87.5	52.5–60.5
DAP neck	133	127		141	98–117.5	76–89
Humerus						
Length	ca 460	–		427–517	402–456	334–408
DTp	180	185		158–190	143–171.5	101.5–132
DAPp	ca 160	–		164–208.5	148.5–190	122–155.5
DTdia.	75	80.5		62–83.5	58.5–70	40–65
DAPdia.	76	77		62–82	64.5–75	47–60
DTd	175	–		164–184	139–157	96–124
DAPd	126	–		118–131.5	110.5–117	82–104
DT tuberosity	167	164		139–180	127–150	103.5–123
Radius						
Length	396	–	353	360–421	328–368	284–329
DTp	118	119	104–110	109–126	103–111	70.5–85
DAPp	77	77.5	62–65	70–82	61–67	43.5–59
DTdia.	55	56	53	49–67	45.5–58	36–44
DAPdia.	40	37.5	35	36–50	30–48.5	23.5–34
DTd	112.5	112	101–106	108–125.5	95–108	72.5–87
DAPd	71	–	66–69	70.5–81.5	58–66	47–55
DTd art.	102	–		96.5–106	87–93	63.5–69.5
DAPd art.	52	–		48–55	41–47	38–43
Ulna						
Length	–	490		442–545	428–467	372–424
DT olecranon	–	81.5		72–97	6305–78	54–67
DAP olecranon	–	123		110–135.5	89–107	74–94
DTp art.	96	98		88–108	82–90.5	56–79.5
DAPp	–	160.5		155–188	137.5–161	110–131.5
DTdia.	50	51		38–53	37.5–41.5	25–35
DAPdia.	54.5	53.5		46–69	40–48	27–36
DTd	–	61		62–110	44.5–57	31–40
DAPd	100	96		91.5–112	67–82	44–61

art: articular; **inf**: inferior; **sup**: superior; **ant**: anterior; **ana**: anatomic.
[a] Data from Beden and Guérin (1973).
[b] Data from Guérin (1980).

medial edge shorter than the lateral one (Fig. 7(F)). The proximal face is quadrangular and formed by two articular facets separated by a smooth sagittal ridge (Fig. 7(H)). The medial facet for the astragalus is wider and longer posteriorly than the external facet for the calcaneus. The posterior edge of the talus facet is very slightly shifted compared to the calcaneus one. The medial face (Fig. 7(G)) has a strong concave posterior edge with a very high posterior part. The antero-superior facet for the navicular is less marked; it is linked by a thin stripe to the postero-superior facet which is fused to the upper postero-medial facet (only observable on the left specimen). The anterior inferior facet for the third cuneiform is well marked and elliptical. The distal edge is straight and a recess is present in the posterior part of the articular complex. The distal face is composed by a rounded square facet for the fourth metatarsal. The anterior edge is convex and the anterior part of the lateral edge is straight due to the facet for the third cuneiform. The lateral face is longer than high and presents a sub-horizontal groove separating the slightly overflowing articular facet for the calcaneus and a strong lateral tuberosity.

Navicular. The navicular is a low, antero-posteriorly concave and latero-medially convex bone. The proximal face is longer than wide (Fig. 7(N)). The shape of the articular surface for the astragalus is very concave and presents a strong recess in the postero-external part. The two third of the lateral edge are not straight but curved due to the presence of a strongly marked antero-lateral outer tip. The lateral face presents a deep depression and the fused facets for the cuboid (Fig. 7(O)). The antero-superior triangular facet, in contact with the upper margin of the bone, is joined by a thin facet to the postero-medial facet, which occupies the full height of the bone.

Third cuneiform. Only the right third cuneiform is preserved; it is low and wide, L-shaped in proximal (Fig. 7(P)) and distal views, with a strong constriction on the medial edge. The proximal face is composed only by the articular surface for the navicular; no postero-lateral process is developed. The lateral face shows two semicircular facets for the cuboid, separated by a deep notch. The medial face presents two distal facets for the second metatarsal and a proximal facet for the second cuneiform occupying the majority or the proximal edge of the face (Fig. 7(Q)).

Second cuneiform. The second cuneiform is represented by the right specimen. The proximal face presents a drop-shaped outline (Fig. 7(S)), composed mainly by the articular surface for the navicular with a posterior expansion forming the facet for the first cuneiform. The medial face presents two-fused facet for the third cuneiform; the anterior one reaches both the proximal and the distal edge of the bone (Fig. 7(T)).

First cuneiform. The first cuneiform (Fig. 7(R)) presents a laterally projected distal tuberosity. The anterior face presents two articular facets, a superior rounded-shape facet for the navicular, and a small distal facet for the second cuneiform.

Second metatarsal. This bone shows a marked torsion at its proximal epiphysis (Fig. 8(C)). The articular surface for the second

Table 3
Comparative measurements (in mm) of carpal bones of *Rhinoceros unicornis* from Kanchanaburi (Thailand) and from extant and fossil Asian rhinoceros specimens.

	Fossil			Extant[b]		
	R. unicornis Kanchanaburi		*R. sondaicus guthi* Phnom Loang[a]	*R. unicornis*	*R. sondaicus*	*D. sumatrensis*
	Left	Right				
Scaphoid						
Length	90	89	78–81	79–90.5	78.5–88	64.5–79.5
Width	65	65	56–62	58.5–63.5	54–65	38–53.5
Height	71	71	63–71	69.5–76	61–69.5	51–58.5
Lenght art. sup.	53	52.5	53–54	53–58	44.5–64	37–46.5
Width art. sup.	63	62	50–60	51.5–60	53–59.5	36–45
Lenght art. inf.	78	77	67–70	76–78.5	63.5–71	51–62
Width art. inf.	38	39	31–33	37–40	31.5–36.5	21–31.5
Semilunar						
Length	72	72.4	71–75	73–81	62–67.5	51.5–58
Width	56	55.8	49–51	55–63.5	47–54.5	35–40
Height	56.5	–	53–62	55–59.5	49.5–54	42–45.5
Height ant.	55.5	–		62–66	52–55	43–45
Pyramidal						
Length	49	47	39–40	46.5–53	35–45	31–35
Width	63	61	51–53	58–68	51.5–57.5	43–49
Height	57	55	57–51	62–70	47.5–55	40–47
Pisiform						
Length	70	–	56	70–82.5	64.5–73.5	49–53
Width	50	50	45	48–52.5	43.5–49.5	32–35
Height	33.5	32.5	23	31–36.5	26–30	22–24
Trapezoid						
Length	53	52.5	43–48	52–54	42–48	35–45
Width	34.8	35	31–33	33–37.5	29–35.5	24.5–28
Height	41	40	33.5–34	40–42.5	32.5–36	30–33.5
Magnum						
Length	98	–	75–81	95–108	85.5–100	69–77.5
Width	54.3	54.1	51–54	56.5–81	48–53.5	34–44.5
Height	74	73	59–61	66–75	60–65	50.5–54.5
Height art.	70	68		66–74	56–65	50–54.5
Uncinate						
Length	100.3	100	90–94	97.5–112	83–92	65.5–78
Length ana.	86.7	86.1	66–68	75.5–86.5	65–74.5	48–63
Width	79	78	67–72	74.5–82.5	60–74	52–61
Height	57.5	57.5	50–57	51.5–59	47.5–55	41–50.5

DT: transverse diameter; **DAP**: anteroposterior diameter; **p**: proximal; **dia**: diaphysis; **d**: distal; **art**: articular.
[a] Data from Beden and Guérin (1973).
[b] Data from Guérin (1980).

cuneiform is long and broad, with a kidney-shape due to the small depression on the lateral edge (Fig. 8(F)). This small groove separates the two facets, composed of two distinct parts, a proximal and a distal one, for the third cuneiform and the third metatarsal, respectively (Fig. 8(L)). The anterior one is vertical and rounded; the posterior one is elliptical and upward. The subdivision of the facet for the third metatarsal and the third cuneiform is not marked. The anterior edge presents a straight outline in medial view (Fig. 8(I)). The section of the diaphysis is circular to quadrangular (Fig. 9).

Third metatarsal. This bone is straight and massive (Fig. 8(B)), with the proximal articular surface wider than long (Fig. 8(E)). The anterior edge of the epiphysis is slightly and regularly concave. Two small articular facets for the second metatarsal are present in medial view (Fig. 8(H)). In lateral view (Fig. 8(K)), the proximal epiphysis shows two articular facets for the fourth metatarsal: an anterior and a posterior one. The anterior one is flat and is triangular in shape; the posterior one is more elliptical and slightly concave. They are separated by a deep groove. The anterior facet is more stretched vertically than the posterior one. The middle section of the diaphysis corresponds to a thick ellipse with the posterior part slightly depressed (Fig. 9).

Fourth metatarsal. The fourth metatarsal presents an arched lateral edge (Fig. 8(A)). The articular surface for the cuboid occupies substantially all of the superior part of the epiphysis; the outline is sub-circular to quadrangular with a notch on the posterior edge (Fig. 8(D)). The postero-proximal tuberosity is pad-shaped and continuous but less developed. The lateral face of the proximal epiphysis is not regularly convex, the top of the convexity lying in the rear part of the face (Fig. 8(J)). On the medial face two articular facets can be observed, corresponding to the third metatarsal (Fig. 8(G)). The anterior facet is trapezoidal and stretched along the edge of the proximal articular surface. The second one is bigger than the first, anterior one and presents a globular-rounded shape. The two facets are separated by a narrow depression. The crest present on the upper half of the medial edge of the shaft is strong and visible. The section of the shaft is elliptical (Fig. 9).

Phalanges. Phalanges are not part of a major focus in rhinoceros studies. Few studies have given description of them for Asian species (Beden and Guérin, 1973). Their dimensions are provided in the supplementary data (Table S1, Appendix A).

Remarks: *Rhinoceros sinensis* is considered as a junior synonym of *Rhinoceros unicornis* (Antoine, 2012).

Morphological and biometrical comparisons. The specimen from Kanchanaburi may be assigned to *Rhinoceros unicornis* based on the following features. Dental characters are equivalent for the molars with those of the Indian species: presence of a strong crochet on the upper molars, development of a crista and a protocone constriction clearly marked on the M1. The crista and the protocone constriction are always absent on the upper molars of *Rhinoceros sondaicus* (Flower, 1876; Colbert, 1942;

Table 4
Comparative measurements (in mm) of metacarpal bones of *Rhinoceros unicornis* from Kanchanaburi (Thailand) and from extant and fossil Asian rhinoceros specimens.

	Fossil					Extant[d]		
	R. unicornis Kanchanaburi		*R. sondaicus guthi* Phnom Loang[a]	*R. fusuiensis* Yangliang[b]	*R. kendengindicus* Kedung Brubus[c]	*R. unicornis*	*R. sondaicus*	*D. sumatrensis*
	Left	Right						
Mc II								
Length	175	175	166–176	ca.150		159.5–187	150–167	128.5–151
DTp	51	50.5	40–44	36.2		42–53	39.5–53	32–40
DTp bis	54	54				42.5–59.5	45–57	32.5–42.5
DAPp	48	49	43–48			46.5–58	43–51.5	33–44
DTdia.	44.5	44	37–43	35		36.5–45.5	39–45.5	29–38
DAPdia.	26	25.5	21–23	20		22–30	18.5–24	15.5–23.5
DTd max.	52	51	46–54	43		47–62	45–56.5	40–47
DT art.	45	44.5	41–48	35.5		42–52	39.5–48	31–40.5
DAPd	45.5	45	42–43	38		41–51.5	36–44.5	32–41.5
Mc III								
Length	211	209	186–207			189–219	175–189	154–180
DTp	71	–	63–68		70	68–74	63–71	49–58
DAPp	59	57	47–53		50	53–65	46–53.5	39.5–48
DTdia.	63	63.5	54–64	46.7	57	54–66	55–66	38–50.5
DAPdia.	25.5	25.5	19–24	21.7	23	24.5–34	19–24	14.5–19
DTd max.	75	75	64–78	54.5		71–82	63.5–74.5	51–62
DTd art.	64	62	52–57	46		60–69	51–60	40.5–48.5
DAPd	50	50	43–50	37.2	45	50–54	41.5–46	30–44
Mc IV								
Length	170	–	147–161	153–155		151.5–178.5	136–153	118–146
DTp	53	51.2	47–51	43.3–49		49–62.5	45–56	34.5–44.5
DAPp	53	53.9	38–44	40–40.6		44–54	41–48	34.5–43
DTdia.	38	–	36–44	37		34–43	38–45	23.5–31
DAPdia.	23.6	–	21–24	20–22		21.5–29	20–23	14–26
DTd max.	58.4	–	45–51	45–48		48–61	46–55	38–46.5
DTd art.	46	–	41–48	40.8–41		45–53.5	42–51	36–42
DAPd	44	–	40–43	35.5		38–45	37.5–51	33–43

DT: transverse diameter; **DAP**: anteroposterior diameter; **p**: proximal; **dia**: diaphysis; **d**: distal; **art**: articular; **max**: maximum.
[a] Data from Beden and Guérin (1973).
[b] Data from Yan et al. (2016).
[c] Data from Hooijer (1946).
[d] Data from Guérin (1980).

Guérin, 1980; Laurie, 1982; Antoine, 2002). The profile of the ectoloph is not flat as noted by Colbert (1942) or cited by Laurie et al. (1983), but presents a sinuous profile (Pocock, 1944; Guérin, 1980) showing two broad undulations, with a more extended one for the metacone rib (Fig. 2; Fig. S2, Appendix A). The antero-external angle of the upper molars does not show a strong bilobation (parastyle buttress) like in *R. sondaicus* (Pocock, 1944; Colbert, 1942; Guérin, 1980). The molar dimensions are in the variation range of extant *R. unicornis* and *R. sinensis* from Yenchingkou, but larger than the *R. sinensis* from Longgudong (Zheng, 2004) and *R. kendengindicus* (Hooijer, 1946) and extant and fossil *R. sondaicus* (Guérin, 1980; Beden and Guérin, 1973; Bacon et al., 2008a; Table 1).

The skull is too poorly preserved to offer diagnostic morphological characteristics, nevertheless the width of the palate, measured between P4 and M1 (86 mm) is close to the variation range observed on extant species (Guérin, 1980): *Rhinoceros unicornis* (88-120 mm), *R. sondaicus* (79-107.5 mm), and *Dicerorhinus sumatrensis* (73.5-95 mm). The mandible presents an inferior border with a straight and slightly oblique outline in the anterior part (Guérin, 1980; Antoine, 2002). The strong backward extension of the alveolus of the lower lateral incisors (Hooijer, 1946; Tong and Guérin, 2009) are encountered in Asian rhinoceros (*R. unicornis* and *R. sondaicus*) whereas the central incisors are absent and the lateral incisors are very reduced for *D. sumatrensis* (Groves, 1983; Tong and Guérin, 2009). The mental foramen below p2 is pronounced, contrary to the small mental foramen of *D. sumatrensis* (Tong and Guérin, 2009). The dimensions of the mandible are in the variation range of *R. unicornis* and larger than the dimensions observed on *R. sondaicus* and *D. sumatrensis* (Table S2, Appendix A).

Rhinoceros unicornis is less well documented in fossil assemblages than its sister species *Rhinoceros sondaicus*. The general skeletal morphology of these two rhinoceros species is similar (Guérin, 1980; Antoine, 2002); the main differences are the size of the postcranial elements, larger for *R. unicornis*. The characteristics of the postcranial elements for this species is mostly known from the work of Guérin (1980) on extant specimens (see also Cuvier, 1804; Osborn, 1898; Hooijer, 1946; Antoine, 2002). Even if the general morphology and biometry of the bones from Kanchanaburi are similar with those of their extant counterpart, some of them show differences. The intermediate tubercle of the humerus enclosed by an elongated and medially hooked greater tubercle (Cuvier, 1804; Groves, 1983; Laurie et al., 1983), has a central position rather than a lateral position as observed on *D. sumatrensis* (Guérin, 1980). The posterior edge of the external surface of the proximal radius shows a strong obliquity, contrary to the observations made by Guérin (1980). The ulna presents a strongly developed olecranon lateral tuberosity and a considerably elongated cranial edge at the top, whereas in *R. sondaicus* the tuberosity is not marked (Guérin, 1980) and the thickening of the cranial border is lighter. The articular surface for the pyramidal is concave and a small articular facet for the semi-lunar is present on both specimens. This character has been observed by Hooijer (1946) on a *R. sondaicus* specimen from Kedung Brubus (Coll. Dub. n°8931 and 9137). It was never observed on the ulna of *R. unicornis* or *R. sondaicus* studied by Guérin (1980), but has been reported by

Table 5
Comparative measurements (in mm) of hindlimb bones of *Rhinoceros unicornis* from Kanchanaburi (Thailand) and from extant and fossil Asian rhinoceros specimens.

	Fossil				Extant[c]		
	R. unicornis Kanchanaburi		*R. sondaicus guthi* Phnom Loang[a]	*R. kendengendicus* Kedung Brubus[b]	*R. unicornis*	*R. sondaicus*	*D. sumatrensis*
	Left	Right					
Femur							
Length	–	515			500–602	410–496	384–466
DT head	–	113			104–112	85–97.5	70–85
DAP head	–	101			101–107	81–92	66.5–78
DTp	–	–			210–248	182–208	140–171
DT 3rd trochanter	–	172	ca.140		154–181	134.5–164	103.5–125
DTdia.	–	84	69	78	71–86.5	62–74	49–65
DAPdia.	58	57	53.5	61	64–70	58–70	43–57
DTd	160	159			151–169.5	135–157	117–129.5
DAPd	185	182			182–206.5	154–172.5	128–155
Height 3rd trochanter	–	83			91–143	73–102	44–70
Patella							
Length	109.5	109.5	107		106–119	97.5–110	81–91
Width	93.5	100	85		90–108	88–97.5	70–83
Height	50	57.5	53		46.5–55.5	48.5–53.5	38–46
Tibia							
Length	395	390	333		376–439	317–357	289–347
DTp	146.35	148.9	117–121		132–151	120–133.5	94.5–117.5
DAPp	–	151	115–121		143–155.5	121–139	84–117
DTdia.	68	69	56–59		65–77	54–61	41–53.5
DAPdia.	64	66	50		52–65	50.5–60	35–48
DTd max.	118.5	116.5	101		112–125.5	95–111	77–93
DAPd max.	78	79.5	71		77–87	68–80	51–66.5
DTd art.	88	90			96	75.5–84.5	63
DAPd art.	66	–			73	59–66	51.5

DT: transverse diameter; **DAP**: anteroposterior diameter; **p**: proximal; **dia**: diaphysis; **d**: distal; **art**: articular; **max**: maximum.
[a] Data from Beden and Guérin (1973).
[b] Data from Hooijer (1946).
[c] Data from Guérin (1980).

Antoine (2002) as a discriminating feature. On the scaphoid the difference of height between the anterior and the posterior part is not so marked (63 *vs*. 65 mm) as observed on extant specimens (Guérin, 1980; Antoine, 2002); the articular surface for the radius presents a trapezoidal outline compared to the triangular shape observed on *R. sondaicus* (Guérin, 1980). The semilunar presents a small articular facet for the ulna, which is absent in extant specimens (Guérin, 1980; Antoine, 2002). The pyramidal present a squared rather than triangular articular surface for the uncinate, as observed in *D. sumatrensis* (Guérin, 1980). The distal edge of the uncinate do not present a depression on the anterior face (Guérin, 1980); only the left specimen presents a very small notch. The contact between the articular surface for the pyramidal and the fifth metacarpal exists; it is less marked in *R. sondaicus* (Heissig, 1972; Guérin, 1980; Antoine, 2002). The proximal epiphysis of the second metacarpal is formed by a large articular surface for the trapezoid; this facet is less developed in *R. sondaicus* (Guérin, 1980). The angle made by the contact between the facet for the magnum and the third metacarpal is well marked, contrary to Guérin's (1980) observations. The diaphysis shows an elliptical medial section similar to *R. unicornis* as figured by Guérin (1980), compared to the quadrangular section of *D. sumatrensis* and the flatter elliptical section of *R. sondaicus* (Beden and Guérin, 1973; Guérin, 1980). On the third metacarpal the articular surface for the magnum overflows on the anterior face as in *R. sondaicus* (Antoine, 2002). The section of the shaft is elliptical, wide and flat with a sharper lateral edge, whereas the lateral and medial edge are more squared for *D. sumatrensis* and the section is much flatter for *R. sondaicus* (Beden and Guérin, 1973; Guérin, 1980). The section of the diaphysis of the fourth metacarpal is a regular thick ellipse compared to the trapezoidal shape observed in *D. sumatrensis* and the squared and sharp lateral and medial edges of *R. sondaicus* (Beden and Guérin, 1973; Guérin, 1980). The difference in height of the eminences on the proximal epiphysis of the tibia is characteristic of the Asian rhinoceros (Cuvier, 1834; Guérin, 1980). Contrary to the observations on extant *Rhinoceros unicornis* (Guérin, 1980), the posterior edge of the talus facet of the cuboid is at the same level than the calcaneus one; on the second metatarsal the passage of the facet for the third metatarsal and the third cuneiform is smooth, and the lateral face of the fourth metatarsal proximal epiphysis is not irregularly convex. Compared to *R. sondaicus*, the middle section of the third metatarsal diaphysis is more rounded and the lateral edge of the fourth metatarsal diaphysis is less curved (Guérin, 1980).

The metric comparisons (Tables 2–7; Tables S1, S2, Appendix A) are mostly done with extant rhinoceros cranial and postcranial specimens from Guérin (1980), and some few postcranial specimens from Asian fossil rhinoceros (Hooijer, 1946; Beden and Guérin, 1973; Yan et al., 2016). Based on these comparisons, *Rhinoceros unicornis* from Kanchanaburi does not differ from a biometric point of view from extant *R. unicornis*, with bone sizes falling in the variation ranges observed in both male and female individuals (Guérin, 1980). The metric values of the bones are not larger than the larger-sized specimens and are very close to the average values observed for extant specimens as well as for the fossil specimens of *R. kendengindicus* (Hooijer, 1946). On the other hand, they are significantly larger than the dimensions observed for extant *R. sondaicus* and *D. sumatrensis* (Hooijer, 1946; Groves and Guérin, 1980; Guérin, 1980) and fossil *R. sondaicus guthi* (Beden and Guérin, 1973) and *Rhinoceros fusuiensis* (Yan et al., 2016). Although only one specimen cannot encompass the complete size variation of the fossil forms of *R. unicornis*, it suggests that probably there has been no change in the body size proportions of this species in Southeast Asia between the late Pleistocene and Holocene times (Fig. 10).

Table 6
Comparative measurements (in mm) of tarsal bones of *Rhinoceros unicornis* from Kanchanaburi (Thailand) and from extant and fossil Asian rhinoceros specimens.

	Fossil					Extant[d]		
	R. unicornis Kanchanaburi		*R. fusuiensis* Yangliang[a]	*R. sinensis* Renzidong[b]	*R. sondaicus guthi* Phnom Loang[c]	*R. unicornis*	*R. sondaicus*	*D. sumatrensis*
	Left	Right						
Astragalus								
DT	112	110			86–100	103.5–112	87.5–100	67.5–87
Height	92	91			78–85	89–101	75–86.5	64.5–77
DAP medial	67	69			57–69	64–70.5	55–63	42.5–58
DTd art.	92.9	97			75–88	85–93	69–84.5	53–67
DAPd art.	54	54			45–46	51–57	42.5–49	34–46.5
D trochlear lips	77	76			63–71	70–79	53–70	50–58
DTd max.	96.5	98			78–91	90.5–102.5	76–89	57–73
Calcaneum								
Height	146	146.5	100	132	127–136	136.5–160	119.5–138	95–117.5
DAP top	–	83			61–70	72.5–85	65.5–77.5	50–61
DAP beak	–	87.5	51		71–76	80.5–92	67.5–74.5	52–62
DT sustentaculum	–	82	57	67	72–80	74–91	73–88.5	58–71
DT top	–	66.5	34	65	46–53	59–72.5	45.5–55	35–46
DT min. posterior	46	44	27		30–35	39–41	28–35	22.5–31
Navicular								
Length	74	72.4			67–73	69–80	64–70	48.5–54.5
Width	63	61			50–54	56.5–62.5	46–54	42–46
Height	33.8	36.1			28–33	37.5–45	26–32	24–29.5
Cuneiform III								
Length	–	56			50	53.5–61	48–60.5	38.5–46
Width	–	52.4			50–51	50.5–57	46.5–53	38–43.5
Height	–	38.1			26	32.5–41	26.5–30.5	25–31.5
Cuneiform II								
Length	–	39.55				38–40.5	36.5–41.5	
Width	–	27				26–26.5	22–25	
Height	–	24.5				22–23	17–23	
Cuboid								
Length	84	83.7			66–75	79–89	69–77	53.5–61.5
Width	52	51			45–50	48–56	42–53	35.5–47.5
Height	–	60			53–56	64–77	48–60	47–60.5
DTp. art. surf.	53	57			43–50	47–58.5	47–54	32.5–38
DAPp art. surf.	51	52			42–47	50–64.5	37–48.5	35–42
Height ant.	50	49			41–47	48–53	33–40	35.5–40.5

DT: transverse diameter; **DAP**: anteroposterior diameter; **p**: proximal; **d**: distal; **art**: articular; **max**: maximum; **min**: minimum; **surf**: surface; **ant**: anterior.
[a] Data from Yan et al. (2016).
[b] Data from Jin and Liu (2009).
[c] Data from Beden and Guérin (1973).
[d] Data from Guérin (1980).

Ageing and taphonomy. The biological age of the specimen is estimated on the basis of tooth replacement. On both mandible and maxillary, the P4 and m3 are not erupted. Originally the upper and lower dp4 were present (observations made on pictures taken after the excavation process). According to studies of Asian fossil rhinoceros assemblages (Tong, 2001; Schepartz and Miller-Antonio, 2008) and based on previous work on the African rhinoceros *Ceratotherium simum* and *Diceros bicornis* (Hillman-Smith et al., 1986; Hitchins, 1978; Anderson, 1966; Goddard, 1970), the individual can be classified as a juvenile. The skeleton was discovered resting on its ventral side, the natural shape of the body was preserved and the rib cage did not collapse (Fig. S1, Appendix A). The body was not exposed for a long time at the surface, and natural disarticulation sequence or scavenger removal activities (Lyman, 1994) did not occur between death and burial. The conservation and the anatomical connection of the body correspond to a fast burial event. The cortical surface of the bone is well preserved, and does not show evidence of modifications by taphonomic agent (weathering, anthropic or carnivore predation). *Rhinoceros unicornis* are known to spend up to 60% of each day wallowing, and the access to water/mud is essential for their thermo-regulation and to rid themselves of parasites (Laurie, 1982). The probable cause of death is by starvation or exhaustion due to the trapping of the individual in a mud pool.

5. Discussion

The rhinoceros skeleton found in the Kanchanaburi Province is attributed to the species *Rhinoceros unicornis*. The specimen was a young individual as shown by unerupted lower and upper third molars and unfused proximal epiphyses of the femur. The specimen presents postcranial elements of large size compared to the dimensions of the bones from the two other recent Asian species (*R. sondaicus* and *D. sumatrensis*) but is included in the variation range of extant *R. unicornis*. No differences in the skeletal proportions are observable between this specimen and extant individuals. Although the geographical distribution of *R. unicornis* is confined today to Nepal (Chitawan Valley) and northern India (Assam and West Bengal), it had a wider distribution in the Indian sub-region during the Holocene (Chauhan, 2008; Rookmaaker, 1983; Deraniyagala, 1958). This geographic distribution was even greater during the Pleistocene (Antoine, 2012). The emersion of Sundaland permitted the dispersion of the species up to its most southern latitudes, attested by the discovery by Dubois of *R. unicornis* referred to *Rhinoceros kendengindicus* specimens on the Java Island, at Kedung Brubus and Djetis (Hooijer, 1946). In the northern latitudes of the Indochinese province the presence of *R. unicornis* is confirmed during the early Pleistocene in South China (Tong and Moigne, 2000) and in northern India associated with *Rhinoceros platyrhinus* (Pandolfi and Maiorino, 2016). Its presence

Table 7
Comparative measurements (in mm) of metatarsal bones of *Rhinoceros unicornis* from Kanchanaburi (Thailand) and from extant and fossil Asian rhinoceros specimens.

	Fossil					Extant[d]		
	R. unicornis Kanchanaburi		*R. sondaicus guthi* Phnom Loang[a]	*R. fusuiensis* Yangliang[b]	*R. kendengendicus* Kedung Brubus[c]	*R. unicornis*	*R. sondaicus*	*D. sumatrensis*
	Left	Right						
MT II								
Length	168	166	142–154	137–ca 146		148–175	133–150.5	114–141
DTp	37	38	31–33	26		26–41.5	26.5–41	25.5–33
DAPp	49.6	51	44–45	38		41–50	39.5–50	28.5–41
DTdia.	33	32	30–33	27–31		30.5–35.5	29–37	26–32
DAPdia.	25	28		21–22		23.5–30	21.5–26.5	16.5–23
DTd max.	45.5	46	38–43	38.7–39.7		42.5–50	42–50	35.5–41
DTd art.	44	44	37–38	31–33		35–48.5	33.5–45	23.5–37
DAPd	44	43.5	38	32.1–36		40–45	35–48.5	31.5–40.5
MT III								
Length	195	193	159–163		ca 180	169.5–202	149.5–163	139–160.5
DTp	59	58.8	54–56		60	59–64	51.5–64.5	42–52
DAPp	54.5	56	45		52	51.5–60	42.5–50	34.5–41.5
DTdia.	55	54	49–50		52	47.5–58	51–58	33–45
DAPdia.	26	26.2	19		24	25–30.5	18–28	14–19
DTd max.	68.7	68.9	60–62			66.5–77.5	59–68	48–57
DTd art.	59.5	61	52		57	54.5–63.5	49–56	37–45
DAPd	48	48	42		45	40.5–52	36.5–42	32.5–40.5
MT IV								
Length	165	162	131–132	141–143		137.5–169.5	127.5–142	115–139
DTp	50.6	50.7	41–42	36.7–38.3		47.5–55.5	46–52	34.5–44
DAPp	46	47.5	40	36–37.4		41.5–53	39–48	32–40
DTdia.	36.8	36.2	32	30–33		32–39	30–48.5	20.5–28
DAPdia.	30	27.6	23	25–30		24–31	23–27	18–24.5
DTd max.	46.7	45.7	39	30–40		40–55.5	40.5–47	32–40
DTd art.	45	44.7	37–38	33.6–35.2		37–47	38.5–44	30–40
DAPd	42.6	43.7	35–37	31–37.5		40–44	34–39.5	31.5–42.5

DT: transverse diameter; **DAP**: anteroposterior diameter; **p**: proximal; **dia**: diaphysis; **d**: distal; **art**: articular; **max**: maximum.
[a] Data from Beden and Guérin (1973).
[b] Data from Yan et al. (2016).
[c] Data from Hooijer (1946).
[d] Data from Guérin (1980).

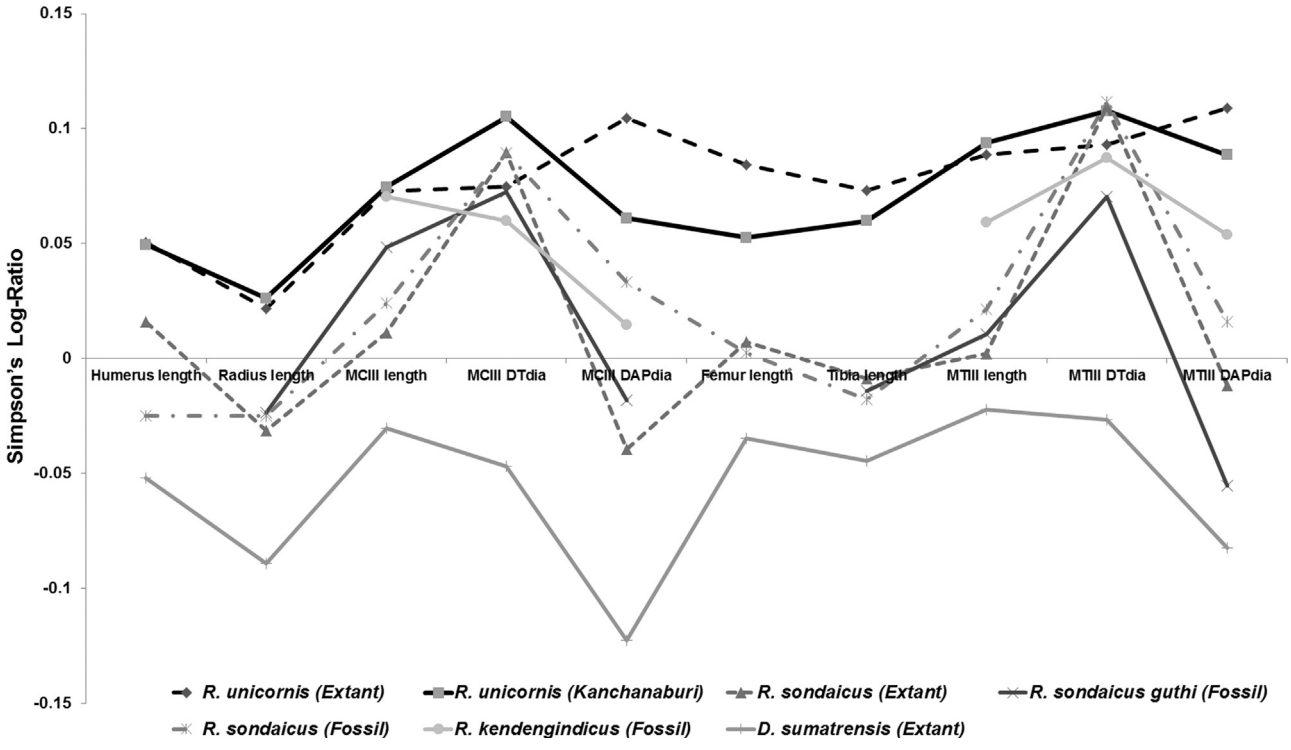

Fig. 10. Simpson's Log-Ratio diagram from skeletal elements of extant and fossil collections of Asian rhinoceros.

was confirmed only for the middle and late Pleistocene in the northern part of the Indochinese sub-region, in northern Vietnam (Cuong, 1985; Olsen and Ciochon, 1990; Bacon et al., 2004, 2006, 2008a), in Laos (Arambourg and Fromaget, 1938; Bacon et al., 2008b, 2011, 2012), in Thailand (Tougard, 1998; Zeitoun et al., 2010; Suraprasit et al., 2016), but also in south China (Colbert and Hooijer, 1953; Kahlke, 1961; Tong, 2000; Antoine, 2012) if we follow the assumption that most of the *R. sinensis* specimens may be referred to *R. unicornis* (Antoine, 2012). *Rhinoceros sinensis* is a near relative of the true rhinoceros and occupied an intermediate position between *R. unicornis* and *R. sondaicus* both in size and morphological characters, perhaps nearer the former than the latter (Matthew and Granger, 1923; Colbert and Hooijer, 1953; Tong and Guérin, 2009). Nevertheless, it has become a wastebasket species (Tong, 2001; Antoine, 2012) within which most of the rhinoceros remains discovered in Pleistocene South China, India and Pakistan have been placed. Some of them were reassessed, as the *R. sinensis* material from Rhino Cave identified now as *Stephanorhinus kirchbergensis* (Tong and Wu, 2010). Only a complete revision of *R. sinensis* material will confirm if it is a congeneric species of *R. unicornis* or if it only represents a junior synonym of *R. unicornis*.

The discovery of this subcomplete skeleton of Indian rhinoceros contributes to a better knowledge of the distribution of this taxon during the late Pleistocene in the Indochinese province and especially in Thailand. It seems that the distribution of *R. unicornis* during the Pleistocene underwent a northward reduction, probably caused by climatic and environmental changes. This led to the extinction of this species during the Holocene in the Indochina subregions and the preservation of only small populations in the Northern Indian subregion. The reduction of its geographic range seems to have been gradual during the Pleistocene. Based on the correlation of the presence of human and rhinoceros remains in archaeological sites, Tong (2000) concluded that human activities induced a rapid decline of the rhinoceros at the end of the late Pleistocene in China. The number of discoveries is very low and does not enable us to follow precisely the evolution of *Rhinoceros unicornis* during the Pleistocene nor to establish with any confidence the various factors (environmental and human) that may have led it to decline. Very few fossil remains from *R. unicornis* have been discovered in Southeast Asia and taphonomic processes (heavy monsoon rain and weathering destruction) that occur in this part of the world must be taken into consideration. Even though this discovery was in an open-air site, most rhinoceros remains have been found in caves, which generally have better preservation than open-air sites. However open-air environments and especially alluvial plains, riverine grasslands, riverine woodlands and swampy areas correspond to the *Rhinoceros unicornis* range habitat (Laurie, 1983). To date, these factors combined with the few studies conducted so far in this large area probably explain the low quantity of data available for this species during the Pleistocene.

6. Conclusions

The characteristics and dimensions of the rhinoceros specimen found in the late Pleistocene deposits of the Kanchanaburi Province are referred to *Rhinoceros unicornis*. The specimen represents the most complete Pleistocene skeleton of Indian rhinoceros found in Southeast Asia. Although the presence of the species has been recognized in some Southeast Asian fossil mammal assemblages, mainly in the form of isolated remains, data concerning the postcranial skeleton were still missing. The present study thus provides a useful set of data for future researches on the evolutionary trends of the rhinoceros lineage during the Pleistocene in Asia. It also confirms the wide geographic distribution of *Rhinoceros unicornis* until the late Pleistocene, especially in the Eastern part of Southeast Asia.

Acknowledgments

The authors are grateful to Suree Teerarungsigul, Director of the Siridhorn Museum, and Phorphen Chantasit who facilitated the study of the collection in their institution. We thank two anonymous reviewers and P.-O. Antoine (associate-editor) for constructive comments of an earlier version of the manuscript. The authors also thank Clive Burrett for reviewing the English version of the paper. Thanks to Anne-Marie Moigne for the comments on a first draft of the paper. This work has been supported by Research Grants, annual budget revenues 2555, Mahasarakham University 02/2555, and the Palaeontological Research and Education Centre.

Appendix A. Supplementary data

Supplementary information (including Figs. S1, S2 and Tables S1, S2) associated with this article can be found, in the online version, at https://doi.org/10.1016/j.geobios.2017.12.003.

References

Alekseev, M.N., Takaya, Y., 1967. An outline of the Upper Cenozoic deposits in the Chao Phraya Basin, Central Thailand. S.E. Asian Studies 5, 106–124.
Anderson, J.L., 1966. Tooth replacement and dentition of the black rhinoceros (*Diceros bicornis* Linn). Lammergeyer 6, 41–46.
Antoine, P.-O., 2002. Phylogénie et évolution des Elasmotheriina (Mammalia, Rhinocerotidae). Mémoires du Muséum National d'Histoire Naturelle, Paris (188).
Antoine, P.-O., 2012. Pleistocene and Holocene rhinocerotids (Mammalia Perissodactyla) from the Indochinese Peninsula. Comptes Rendus Palevol 11, 159–168.
Arambourg, C., Fromaget, J., 1938. Le gisement quaternaire de Tam Nang (Chaîne Annamitique septentrionale). Sa stratigraphique et ses faunes. Comptes Rendus de l'Académie des Sciences 203, 793–795.
Auetrakulvit, P., 2004. Faunes du Pleistocène final à l'Holocène de Thaïlande : une approche archéozoologique (Ph. D. thesis). University of Aix-Marseille I (Unpubl.).
Bacon, A.-M., Demeter, F., Schuster, M., Vu, T.L., Nguyen, K.T., Antoine, P.-O., Ha, H.N., Nguyen, M.H., 2004. The Pleistocene Ma U'Oi cave, northern Vietnam: palaeontology, sedimentology and palaeoenvironments. Geobios 37, 305–314.
Bacon, A.-M., Demeter, F., Roussé, S., Long, V.T., Duringer, P., Antoine, P.-O., Thuy, N.K., Huong, N.M., Dodo, Y., Matsumura, H., Schuster, M., Anezaki, T., 2006. New palaeontological assemblage, sedimentological and chronological data from the Pleistocene Ma U'Oi cave (Northern Vietnam). Palaeogeography, Palaeoclimatology, Palaeoecology 230, 280–298.
Bacon, A.-M., Demeter, F., Duringer, P., Helm, C., Bano, M., Vu, T.L., Nguyen, T.K.T., Antoine, P.-O., Bui, T.M., Nguyen, T.M.H., Dodo, Y., Chabaux, F., Rihs, S., 2008a. The Late Pleistocene Duoi U'Oi Cave in northern Vietnam: palaeontology, sedimentology, taphonomy and palaeoenvironments. Quaternary Science Reviews 27, 1627–1654.
Bacon, A.-M., Demeter, F., Tougard, C., De Vos, J., Sayavongkhamdy, T., Antoine, P.-O., Bouasisengpaseuth, B., Sichanthongtip, P., 2008b. Redécouverte d'une faune pléistocène dans les remplissages karstiques de Tam Hang au Laos: Premiers résultats. Comptes Rendus Palevol 7, 277–288.
Bacon, A.-M., Duringer, P., Antoine, P.-O., Demeter, F., Shackelford, L., Sayavongkhamdy, T., Sichanthongtip, P., Khamdalavong, P., Nokhamaomphu, S., Sysuphanh, V., Patole-Edoumba, E., Chabaux, F., Pelt, E., 2011. The Middle Pleistocene mammalian fauna from Tam Hang karstic deposit, northern Laos: new data and evolutionary hypothesis. Quaternary International 245, 315–332.
Bacon, A.-M., Demeter, F., Duringer, P., Patole-Edoumba, E., Sayavongkhamdy, T., Coupey, A.-S., Shackelford, L., Westaway, K., Ponche, J.-L., Antoine, P.-O., Sichanthongtip, P., 2012. Les sites de Tam Hang, Nam Lot et Tam Pà Ling au nord du Laos. Des gisements à vertébrés du Pléistocène aux origines des Hommes modernes. Éditions CNRS.
Beden, M., Guérin, C., 1973. Le gisement de vertébrés du Phnom Loang (Province de Kampot Cambodge). Faune Pléistocène moyen terminal (Loangien). Travaux et documents de l'O.R.S.T.O.M. 27, 1–97.
Chauhan, P., 2008. Large mammal fossil occurrences and associated archaeological evidence in Pleistocene contexts of peninsular India and Sri Lanka. Quaternary International 192, 20–42.
Colbert, E.H., 1942. Notes on the lesser one horned rhinoceros, *Rhinoceros sondaicus*. American Museum Novitates 1207, 1–6.
Colbert, E.H., Hooijer, D.A., 1953. Pleistocene mammals from the limestone fissures of Szechwan, China. Bulletin of the American Museum of Natural History 102, 1–134.

Corlett, R.T., 2010. Megafaunal extinctions and their consequences in the tropical Indo-Pacific. In: Haberle, S.G., Stevenson, J., Prebble, M. (Eds.), Terra Australis 32: Altered Ecologies: Fire, Climate and Human Influence on Terrestrial Landscapes. ANU E-Press, Canberra, pp. 117–131.
Cuong, N.L., 1985. Fossile Menschenfunde aus Nordvietnam. In: Herrmann, J., Ullrich, H. (Eds.), Menschwerdung-Biotischer und gesellschaftlicher Entwicklungsprozess. Akademieverlag, Berlin, pp. 96–102.
Cuvier, G., 1804. Osteological description of the one-Horned Rhinoceros continued. Philosophical Magazine 20 (78), 111–120.
Cuvier, G., 1834. Recherches sur les ossements fossiles, Paris.
Deraniyagala, P.E.P., 1958. The Pleistocene of Ceylon. Ceylon National Museums, Colombo.
Dheeradilok, P., 1995. Quaternary coastal morphology and deposition in Thailand. Quaternary International 26, 49–54.
Falconer, H., 1867. Description of the Plates of the Fauna Antiqua Sivalensis from Notes and Memoranda. Robert Hardwicke, London.
Filoux, A., 2013. Études de restes fauniques provenant des grottes, In: Bellina, B. (Dir.) Mission Archéologique Franco-Thaïe en péninsule Thaï-Malaise, Programme 2011-2014 « Évolution des populations de la péninsule Thaï-Malaise septentrionale et de leurs écosystèmes en relation avec les échanges hauturiers », pp. 44-48.
Flower, W.H., 1876. On some cranial and dental characters of the existing species of Rhinoceroses. Proceedings of the Zoological Society of London 44, 443–457.
Goddard, J., 1970. Age criteria and vital statistics of a black rhinoceros population. East African Wildlife Journal 8, 105–121.
Groves, C.P., 1983. Phylogeny of the living species of Rhinoceros. Zeitschrift für Zoologische Systematik und Evolutionforschung 21, 293–313.
Groves, C.P., Guérin, C., 1980. *Le Rhinoceros sondaicus annamiticus* (Mammalia, Perissodactyla) d'Indochine: distinction taxinomique et anatomique; relations phylétiques. Geobios 13, 199–208.
Guérin, C., 1980. Les rhinocéros (Mammalia, Perissodactyla) du Miocène terminal au Pléistocène supérieur en Europe occidentale. Comparaison avec les espèces actuelles. Documents du Laboratoire de Géologie de Lyon 79, 1–1185.
Hatting, T., 1967. Animal bones from the tombs of the Bang site settlement, Ban Kao. In: Sorensen, P., Hatting, T. (Eds.), Archaeological Investigations in Thailand. Vol. 2, Ban Kao. Part 1. The archaeological materials from the burials. Munksgaard, Copenhagen, pp. 155–164.
Heissig, K., 1972. Paläontologische und geologische Untersuchungen im Tertiär von Pakistan. 5. Rhinocerotidae (Mamm.) aus den unteren und mittleren Siwalik-Schichten. Abhandlungen der bayerischen akademie der wissenschaften mathematisch-naturwissenschaftliche klasse 152, 1–112.
Higham, C.F.W., Thosarat, R., 2004. The excavation of Khok Phanom Di: a prehistoric site in Central Thailand. Volume 7 summary and conclusions (Reports of the Research committee of the Society of Antiquaries of London 62) Society of Antiquaries of London, London, pp. 239–274.
Hitchins, P.M., 1978. Age determination of the black rhinoceros (*Diceros bicornis* Linn.) in Zululand. South African Journal of Wildlife Research 8, 71–80.
Hillman-Smith, K., Owen-Smith, R.N., Anderson, J.L., Hall Martin, A.J., Selaladi, J.P., 1986. Age estimation of the white rhinoceros (*Ceratotherium simum*). Journal of Zoology, London 210, 355–379.
Hooijer, D.A., 1946. Prehistoric and fossil rhinoceroses from the Malay Archipelago and India. Zoologische Mededelingen Museum Leiden 26, 1–138.
Jarupongsakul, S., Hattori, T., Wichaidit, P., 1991. Salinization in the Holocene fan-delta of Maekhlong River, Thailand. Southeast Asian Studies 29, 49–63.
Jin, C.Z., Liu, J.Y., 2009. Paleolithic site-the Renzidong Cave, Fanchang, Anhui. Science Press, China. Beijing (in Chinese with English summary).
Kahlke, H.D., 1961. On the complex of the *Stegodon-Ailuropoda* fauna of Southern China and the chronological position of *Gigantopithecus blacki* V. Koenigswald. Vertebrata Palasiatica 2, 83–108.
Laurie, W.A., 1982. Behavioral ecology of the greater one-horned rhinoceros (*Rhinoceros unicornis*). Journal of Zoology 196, 307–341.
Laurie, W.A., Lang, E.M., Groves, C.P., 1983. *Rhinoceros unicornis*. Mammalian Species 211, 1–6.
Lydekker, R., 1881. Siwalik Rhinocerotidae. Palaeontologia Indica 10 (2), 1–62.
Lyman, R.L., 1994. Vertebrate taphonomy. Cambridge University Press, New York.
Martin, P.S., 1984. Prehistoric overkill: the global model. In: Martin, P.S., Klein, R.G. (Eds.), Quaternary Extinctions: a Prehistoric Revolution. Arizona University Press, Tucson, pp. 354–403.
Matthew, W.D., Granger, W., 1923. New fossil mammals from the Pliocene of Sze-Chuan, China. Bulletin of the American Museum of Natural History 48, 563–598.
Milliman, J.D., Rutkowski, C., Meybeck, M., 1995. River Discharge to the Sea: A Global River Index. LOICZ Core Project Office, 125.
Olsen, J.W., Ciochon, R.L., 1990. A review of evidence for postulated Middle Pleistocene occupations in Viet Nam. Journal of Human Evolution 19, 761–788.
Osborn, H.F., 1898. The extinct rhinoceroses. Memoirs of the American Museum of Natural History 1, 75–164.
Pandolfi, L., Maiorino, L., 2016. Reassessment of the largest Pleistocene rhinocerotine *Rhinoceros platyrhinus* (Mammalia, Rhinocerotidae) from the Upper Siwaliks (Siwalik Hills, India). Journal of Vertebrate Paleontology 36 (2), 1–12.
Pocock, R.I., 1944. Some cranial and dental characters of the existing species of Asiatic Rhinoceros. Proceeding of the Zoological Society, London 114, 437–450.
Rookmaaker, L.C., 1983. The former distribution of the Indian rhinoceros *(Rhinoceros unicornis)* in India and Pakistan. Journal of the Bombay Natural History Society 80, 555–563.
Simpson, G.G., 1941. Large Pleistocene felines of North America. American Museum Novitates 1136, 1–27.
Schepartz, L.A., Miller-Antonio, S., 2008. Taphonomy, Life History, and Human Exploitation of *Rhinoceros sinensis* at the Middle Pleistocene Site of Panxian Dadong, Guizhou, China. International Journal of Osteoarchaeology 20, 253–258.
Suraprasit, K., Jaeger, J.-J., Chaimanee, Y., Chavasseau, O., Yamee, C., Tian, P., Panha, S., 2016. The Middle Pleistocene vertebrate fauna from Khok Sung (Nakhon Ratchasima, Thailand): biochronological and paleobiogeographical implications. ZooKeys 613, 1–157.
Takaya, Y., 1972. Quaternary outcrops of the Southern part of the central plain of Thailand. The Southeast Asian Studies 10 (2), 298–320.
Thosarat, R., Kijngam, A., 2011. The faunal remains. In: Higham, C.F.W., Kijngam, A. (Eds.), The Excavation of Ban Non Wat. Part Two: The Neolithic Occupation. The Thai Fine Arts Department, Bangkok, pp. 170–197.
Tong, H., 2000. Les Rhinocéros des sites à fossiles humains de Chine. L'Anthropologie 104, 523–529.
Tong, H., 2001. Age profiles of rhino fauna from the Middle Pleistocene Nanjing Man site, South China - explained by the rhino specimens of living species. International Journal of Osteoarchaeology 11, 231–237.
Tong, H., Moigne, A.-M., 2000. Quaternary Rhinoceros of China. Acta Anthropologica Sinica 19, 257–263.
Tong, H., Guérin, C., 2009. Early Pleistocene *Dicerorhinus sumatrensis* remains from the Liucheng *Gigantopithecus* Cave, Guangxi. China. Geobios 42, 525–539.
Tong, H., Wu, X.-Z., 2010. *Stephanorhinus kirchbergensis* (Rhinocerotidae, Mammalia) from the Rhino Cave in Shennongjia. Hubei. Chinese Science Bulletin 55, 1157–1168.
Tougard, C., 1998. Les faunes de grands mammifères du Pléistocène moyen terminal de Thaïlande dans leur cadre phylogénétique, paléoécologique et biochronologique, Ph. D. thesis. University of Montpellier II (unpubl.).
Wattanapituksakul, A., 2006. Late Pleistocene mammal teeth from the Tham Lod Rockshelter, Amphoe Pang Mapha, Changwat Mae Hong Son. M. Sc. thesis. University of Chulalongkorn, Department of Geology (unpubl.).
Yan, Y., Wang, Y., Zhu, M., Chen, S., Qin, D., Jin, C., 2016. New Early Pleistocene Perissodactyl remains associated with *Gigantopithecus* from Yangliang Cave, Guangxi of southern China. Historical Biology 28, 237–251.
Zheng, S.H., 2004. Jianshi Hominid Site. Science Press, Beijing.
Zeitoun, V., Lenoble, A., Laudet, F., Thompson, J., Rink, W.J., Mallye, J.-B, Chinnawut, W., 2010. The Cave of the Monk (Ban Fa Suai, Chiang Dao wildlife sanctuary, northern Thailand). Quaternary International 220, 160–173.